Electronic Supplementary Material (ESI) for Chemical Science.
This journal is © The Royal Society of Chemistry 2023

Supplementary Information

Hysteresis Behavior in the Unfolding/Refolding Processes of a Protein Trapped in Metallo-Cages

Takahiro Nakama,[a] Anouk Rossen,[a] Risa Ebihara,[a] Maho Yagi-Utsumi,[b,c,d] Daishi Fujita,[e] Koichi Kato,[b,c,d] Sota Sato,[a] Makoto Fujita*[a,b]

[a]Department of Applied Chemistry, Graduate School of Engineering, The University of Tokyo, Hongo, Bunkyo-ku, Tokyo 113-8656, Japan
[b]Institute for Molecular Science (IMS), 5-1 Higashiyama, Myodaiji, Okazaki, Aichi 444-8787, Japan
[c]Exploratory Research Center on Life and Living Systems (ExCELLS), 5-1 Higashiyama, Myodaiji, Okazaki, Aichi 444-8787, Japan
[d]Graduate School of Pharmaceutical Sciences, Nagoya City University, 3-1 Tanabe-dori, Mizuho-ku, Nagoya 467-8603, Japan
[e]Institute for Integrated Cell-Material Sciences (iCeMS), Institute for Advanced Study, Kyoto University, Yoshida, Sakyo-ku, Kyoto 606-8501, Japan

Correspondence to: mfujita@appchem.t.u-tokyo.ac.jp

Table of Contents

1. Materials and Methods

Instruments and materials

^{1}H–^{15}N HSQC NMR spectra were recorded on a Bruker AVANCE 800 MHz spectrometer equipped with a 5-mm triple-resonance cryogenic probe (800 MHz for ^{1}H NMR and 81 MHz for ^{15}N NMR) at 300K. The NMR data were processed and analyzed using TopSpin (Bruker) and NMRFAM-SPARKY software.[1] The chemical shift values of ^{1}H NMR are with respect to a residual solvent signal for CD_3CN (δ = 1.94 ppm). Solvents and reagents were purchased from Tokyo Chemical Industry (TCI) Co., Ltd., FUJIFILM Wako Pure Chemical Corporation, Kanto Chemical Co., Inc., and Sigma-Aldrich Co. All the chemicals were used without any further purification.

Preparation of CLE

A cutinase-like enzyme (CLE) was prepared as previously described.[2] Briefly, CLE was expressed in Escherichia coli strain SHuffle T7 and purified by Ni-affinity column and gel filtration chromatography. CLE solution was stored in 50% aqueous glycerol at –78 °C.

Preparation of caged CLE **1** and **2**

The stocked solution of CLE was concentrated by ultrafiltration (Amicon Ultra, 10 kDa MWCO (Merck)) to remove glycerol and salts. The CLE solution (0.04 μmol) was mixed with ligand **3** or **4** (2 μmol) in a mixed solvent of CD_3CN and H_2O. After shaking at 20 °C for 2 h, to the mixture was added $[Pd(MeCN)_4](BF_4)_2$ (0.98 μmol for complex **1**, 0.90 μmol for complex **2**) in CD_3CN. The mixture in CD_3CN/H_2O = 1:1 was shaken at 20 °C overnight. The formation of the protein complex was confirmed by ^{1}H and ^{1}H DOSY NMR.

^{1}H–^{15}N HSQC NMR analysis of caged CLE

Prior to the measurement, caged CLE was dialyzed with CD_3CN/HEPES-KOH buffer (pH 7.5, 2 mM) = 1:1 (1 h × 3, Xpress Micro Dialyzer MD300, 3.5 kDa MWCO (Scienova)) to adjust pH. Dialysis filter contents were homogenized by pipetting every 15 mins. After measuring NMR at 50% acetonitrile, the sample was dialyzed with CD_3CN/H_2O = 80:20 (1 h × 3). ^{1}H–^{15}N HSQC spectrum of the dialyzed sample was measured, and consecutive spectra were taken after increasing the CD_3CN ratio 1% at a time by the addition of CD_3CN/H_2O = 90:10. After caged CLE denatured as much as in 90% acetonitrile, NMR spectra were recorded after the acetonitrile content was decreased stepwise by adding CD_3CN/H_2O = 10:90. The sample was left to stand for more than 30 min after CD_3CN/H_2O addition.

The HSQC cross-peaks were assigned based on the triple-resonance NMR experiments in the previous study.[2] Relative cross-peak intensities were determined considering the dilution of the sample. Chemical shift perturbations (CSP) were calculated as follows,

$$\mathrm{CSP\ (ppm)} = [(\Delta\delta_H)^2 + (\Delta\delta_N/5)^2]^{1/2},$$

where $\Delta\delta_H$ and $\Delta\delta_N$ are observed chemical shift changes for ^{1}H and ^{15}N, respectively.

Circular dichroism

CD spectra were recorded on a J-1500 (Jasco) equipped with a Peltier temperature controlling system in a 1 mm quartz cuvette with a screw cap. The spectra of caged CLE **1** and **2** (0.036 or 0.072 mg/mL) were taken after mixing with different ratios of acetonitrile/water solvents.

Dynamic light scattering (DLS)

Measurements were performed on the DynaPro NanoStar (Wyatt Technology) using the DYNAMICS 7.1 software. CLE in more than 80% acetonitrile was prepared in the same way as the NMR samples and filtered through a disk filter. The sample (100 μL) was placed in a disposable microcuvette and was measured at 25 °C for 10 acquisitions (10 seconds each). Solvent parameters: refractive index = 1.343,[3] viscosity = 0.47 cP.[4]

^{1}H diffusion-ordered NMR spectroscopy (DOSY)

^{1}H DOSY NMR spectra were recorded on a JEOL ECZ500 spectrometer (500 MHz) or a Bruker AVANCE III HD 500 MHz spectrometer (500 MHz) at 300 K. The NMR data was processed on Delta (JEOL) or TopSpin (Bruker), and the diffusion coefficient D was calculated. The effective hydrodynamic (Stokes) radius (r) was estimated based on the Stokes–Einstein equation (1)

$$D = \frac{k_B T}{6\pi\eta r} \quad (1)$$

where k_B is the Boltzman constant, T is the temperature in Kelvin, and η is the viscosity of the solution. η is 0.53 cP and 0.49 cP in 80% and 83% acetonitrile/water (v/v), respectively.[4]

2. Unfolding/refolding of caged CLE 1 (CLE@1)

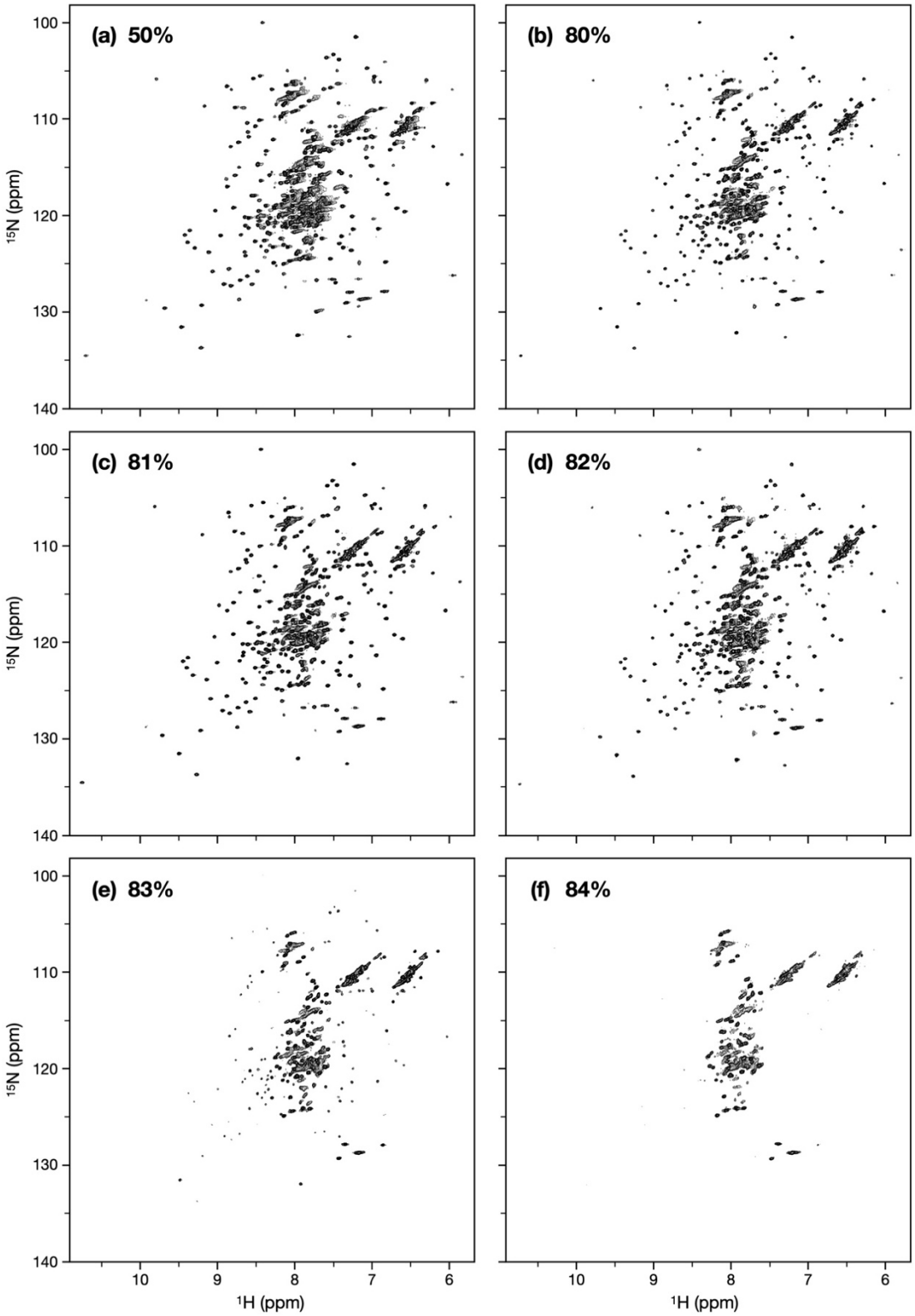

Figure S1 Unfolding of CLE@1. ^{1}H–^{15}N HSQC spectra of unfolding of CLE@**1** with increasing acetonitrile content (800 MHz, 300 K). CD_3CN/H_2O = (a) 50:50, (b) 80:20, (c) 81:19, (d) 82:18, (e) 83:17, (f) 84:16 (v/v). As shown in the previous NMR analysis, CLE maintains the structure after the encapsulation.[2] The native structure of caged CLE **1** was retained from 50% to 82% acetonitrile ratio and suddenly denatured at 83%.

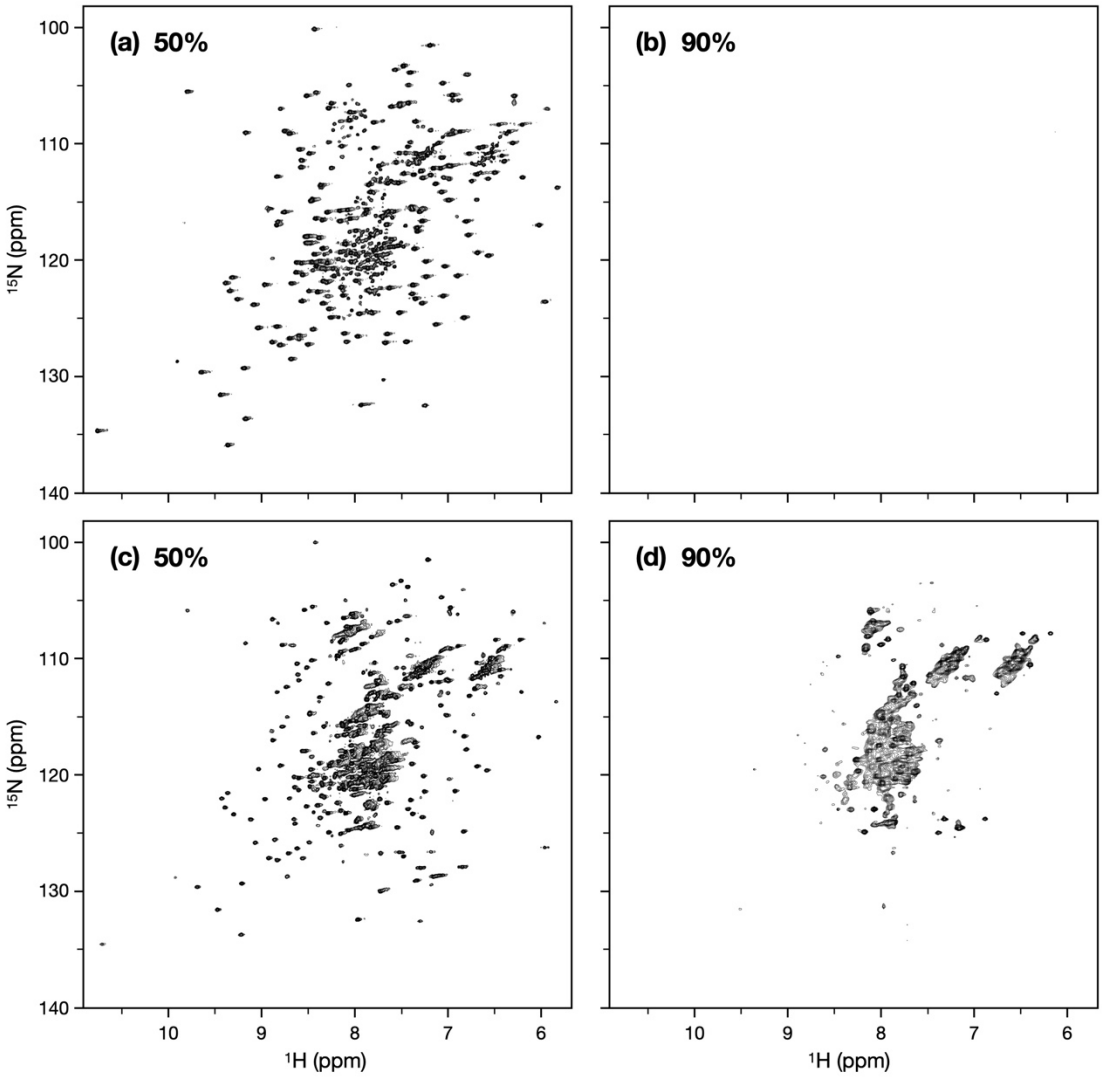

Figure S2 The encapsulation in an $M_{12}L_{24}$ cage suppresses the CLE aggregation. ^{1}H–^{15}N HSQC spectra of (a,b) uncaged CLE and (c,d) caged CLE **1** in acetonitrile/water mixtures (800 MHz (a-c), 600 MHz (d), 300 K). CD_3CN/H_2O = (a,c) 50:50, (b,d) 90:10 (v/v). Uncaged CLE precipitates in more than 50% acetonitrile at any concentration suitable for NMR, and no signals were observed in the high acetonitrile content. On the other hand, the caged CLE does not form any precipitates even in 90% acetonitrile, and its partially unfolded structure can be observed by NMR.

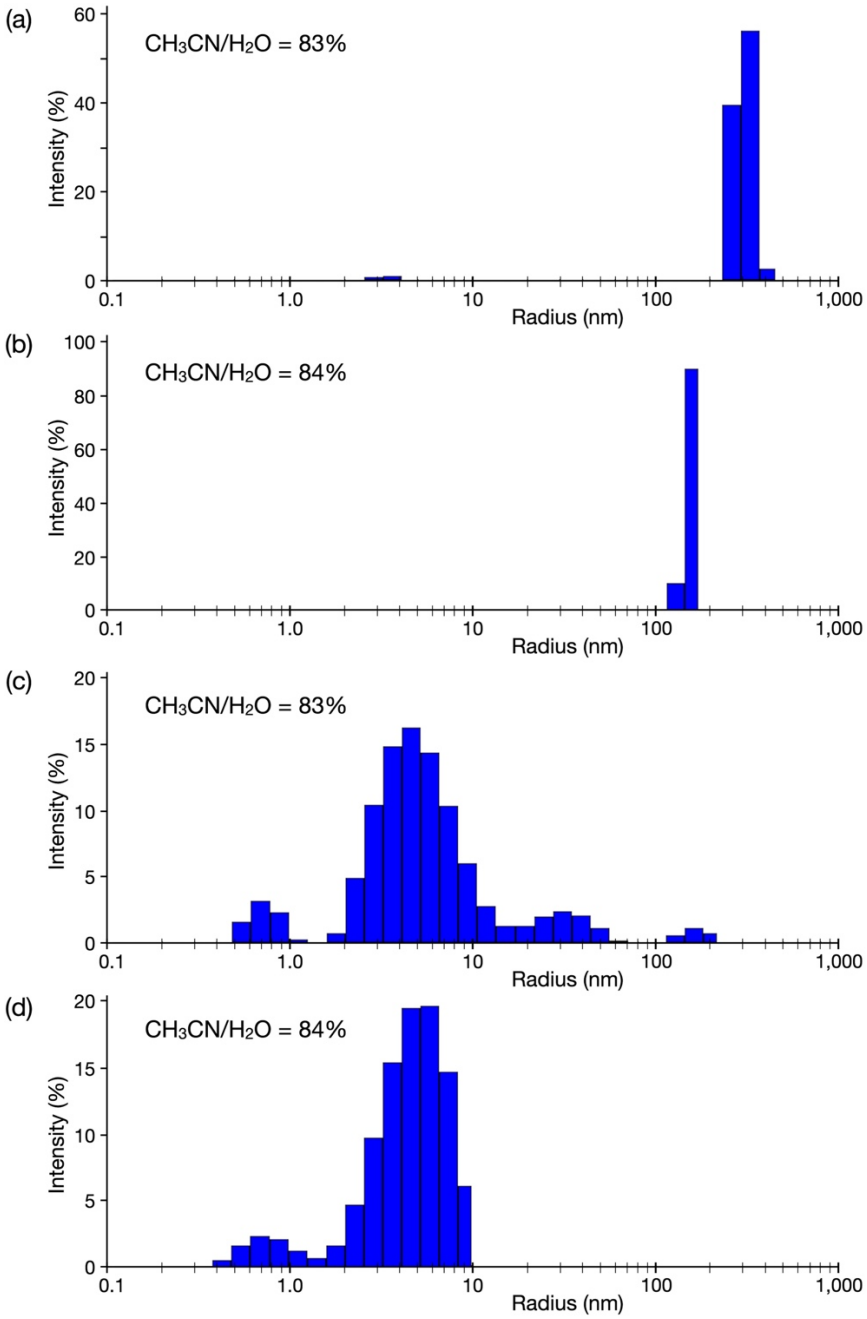

Figure S3 Dynamic light scattering (DLS) of CLE at the unfolding transition point. (a,b) uncaged CLE and (c,d) CLE@**1** in (a,c) 83%, (b,d) 84% acetonitrile/water. Uncaged CLE denatures to form large precipitates, most of which cannot be measured. Not a monomer (radius: ~2.3 nm) but soluble aggregates were observed by DLS. In contrast, caged CLE does not precipitate and remains as a monomeric form. It should be noted that there were less than 0.1% volume of large particles (>10 nm) in the caged protein samples (c,d).

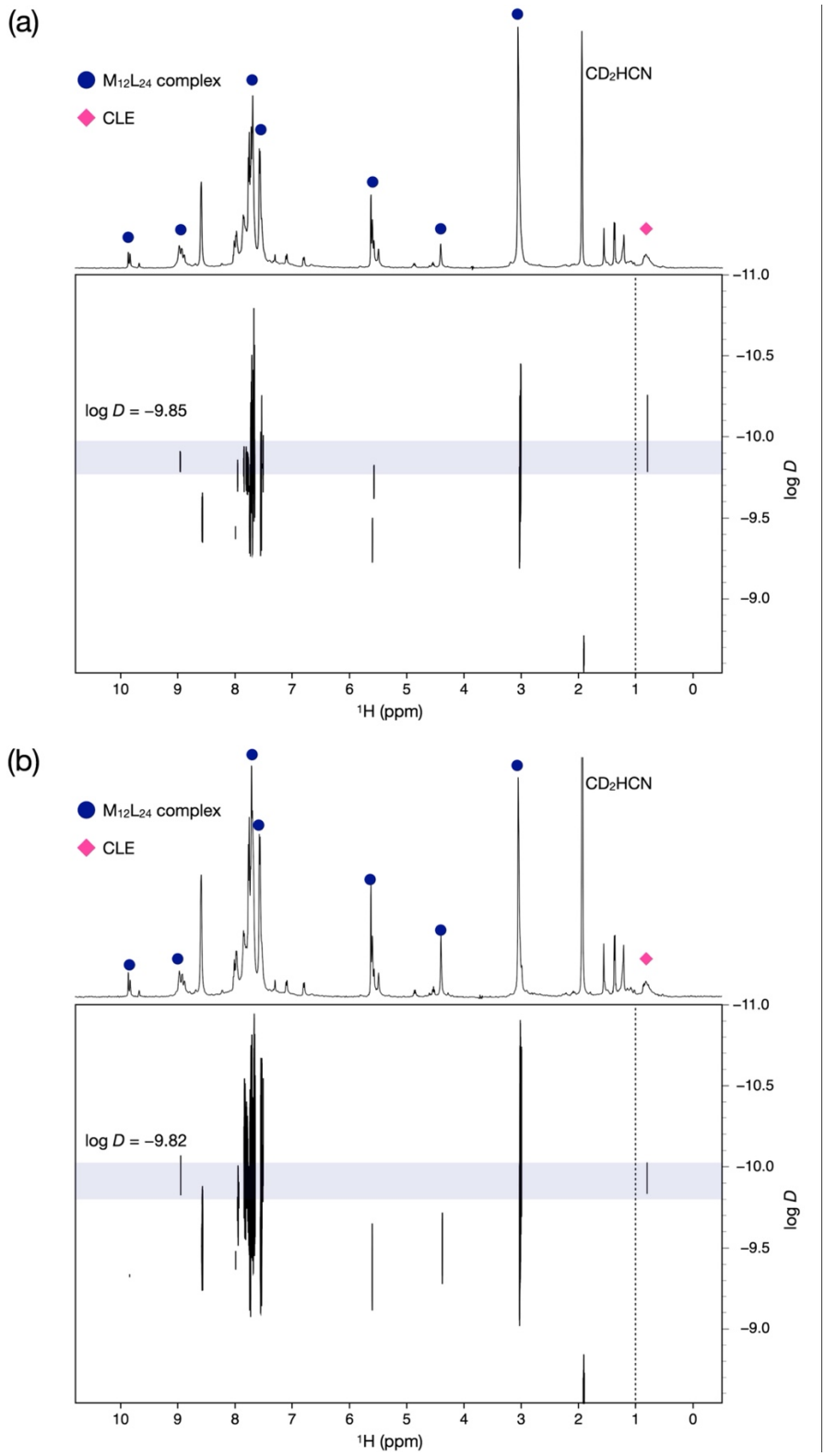

Figure S4 ^{1}H diffusion-ordered NMR spectroscopy (DOSY) NMR spectra of CLE@1. (a) 80% and (b) 83% CD_3CN/D_2O (500 MHz, 300K). Resonances from the $M_{12}L_{24}$ cage and CLE show the same diffusion coefficient *D*. Based on the Stokes–Einstein equation, the estimated radius is 3.0 nm at both ratios, which agrees well with that of the cage (3.1 nm in modeling). This indicates that CLE was encapsulated in the cage and thus prevented from aggregation in high acetonitrile content. The peak intensity of CLE (0-1 ppm) was increased for clarity.

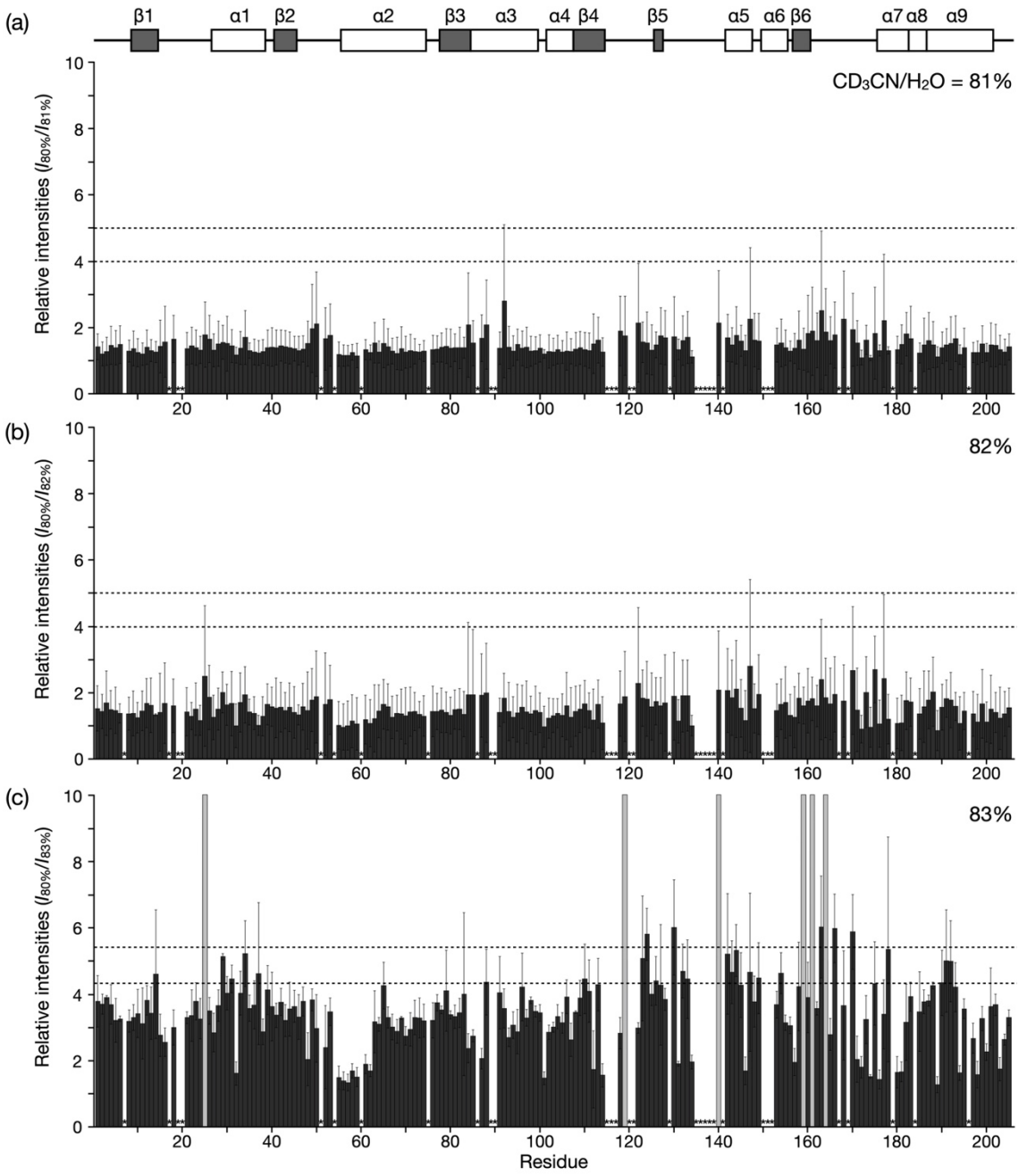
(a)
β1 α1 β2 α2 β3 α3 α4 β4 β5 α5 α6 β6 α7 α8 α9
CD3CN/H2O = 81%
Relative intensities (I80%/I81%)
(b)
82%
Relative intensities (I80%/I82%)
(c)
83%
Relative intensities (I80%/I83%)
Residue

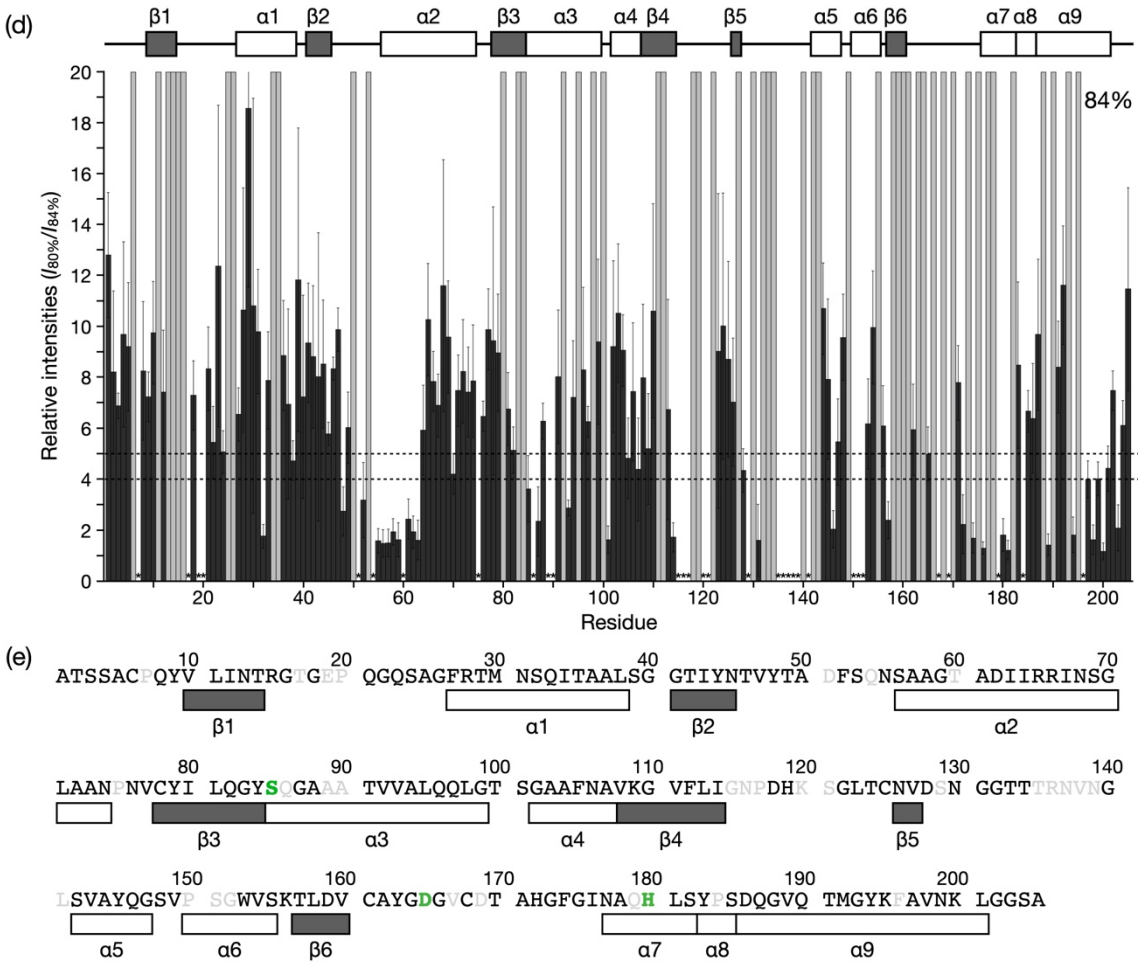

Figure S5 Cross-peak intensity reduction in the unfolding of CLE@1. (a-d) Resonance intensities for each residue of caged CLE **1** relative to those at 80% acetonitrile ratio ($I_{80\%}$). CD_3CN/H_2O = (a) 81%, (b) 82%, (c) 83%, (d) 84%. The intensities were corrected taking into account the dilution of the sample. Error bars represent standard deviation. $N = 3$. Peaks that disappeared in each acetonitrile content are indicated by gray bars. The unassigned residues are denoted with asterisks. (e) Sequence of CLE with its secondary structure. The catalytic triad (S85, D165, and H180) is highlighted in green. The unassigned residues are shown in gray.

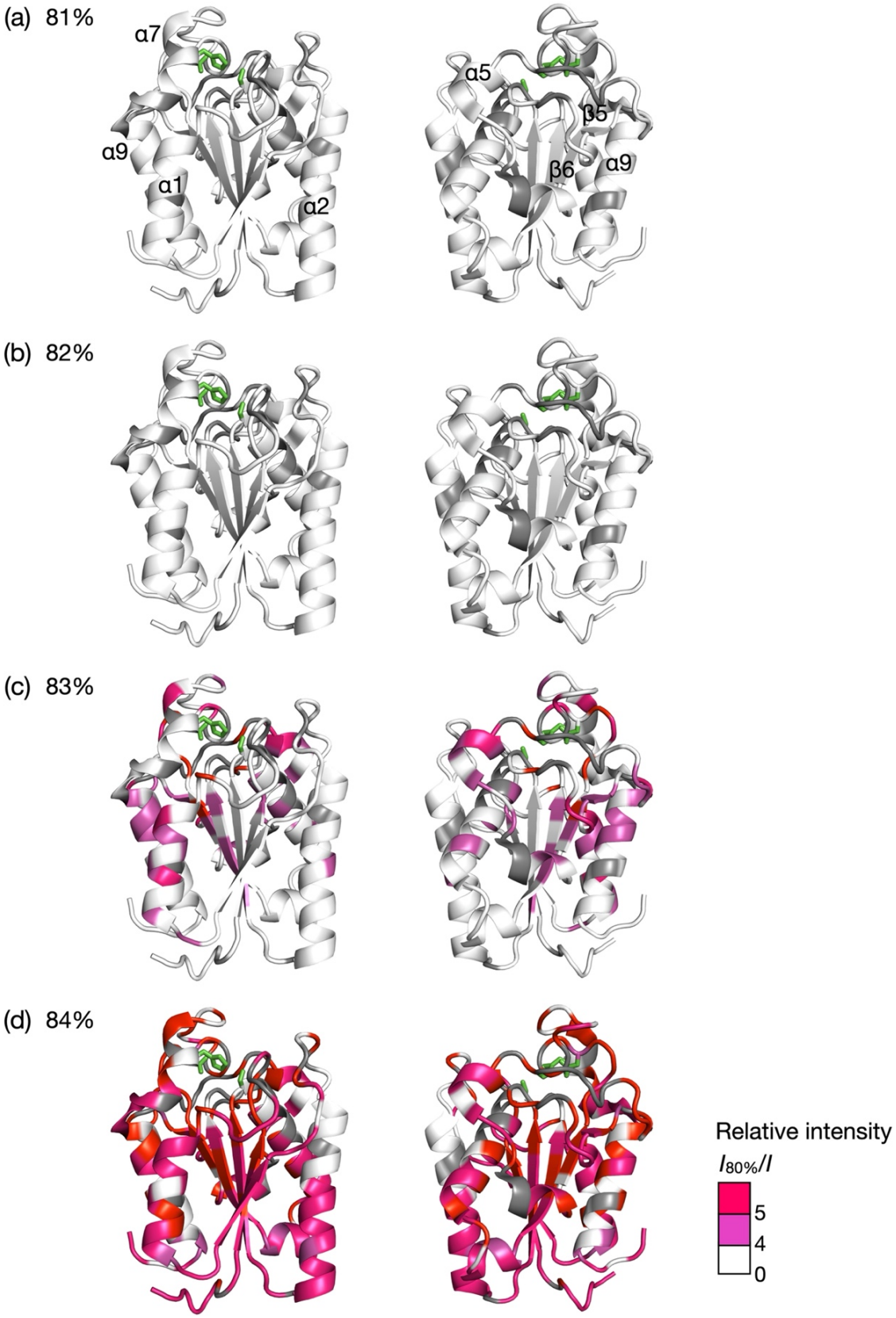

Figure S6 Mapping of the intensity reduction in the unfolding. The relative intensities ($I_{80\%}/I$) at each acetonitrile ratio were mapped on the CLE structure (PDB: 2CZQ). CD_3CN/H_2O = (a) 81%, (b) 82%, (c) 83%, (d) 84%. The catalytic triad (S85, D165, and H180) is highlighted in green. The residues assigned to the disappeared peaks and unassigned residues are shown in red and gray, respectively.

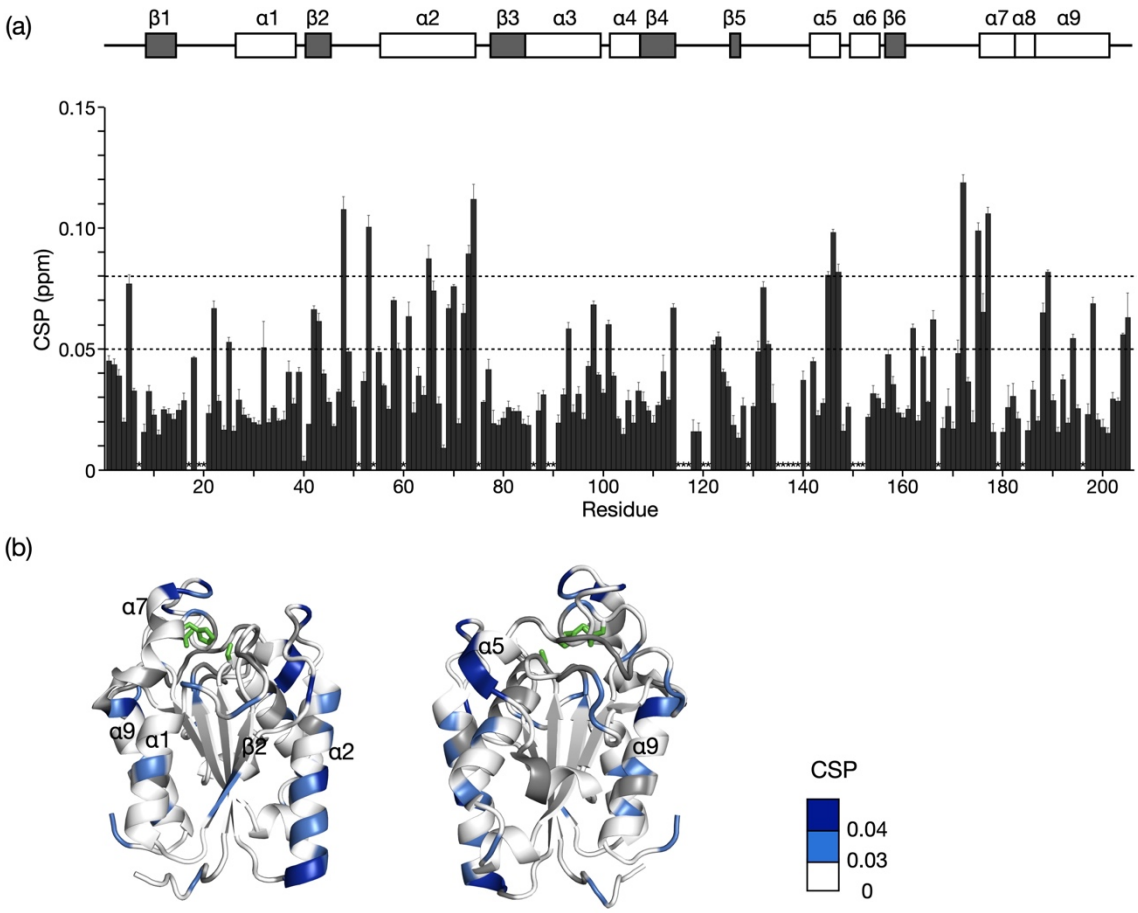

Figure S7 Structural change of CLE after dialysis with 80% acetonitrile. (a) Chemical shift perturbation (CSP) for each residue of caged CLE **1** at 80% acetonitrile content relative to 50%. Error bars represent standard deviation. $n = 3$. The unassigned residues are denoted with asterisks. (b) Mapping of the CSP on the CLE structure (PDB: 2CZQ). The catalytic triad (S85, D165, and H180) is highlighted in green. The unassigned residues are shown in gray. The solvent-exposed helices and loops were perturbed by the solvent exchange. In particular, large CSP was observed in the α2 helix, which retained even at 84% acetonitrile content.

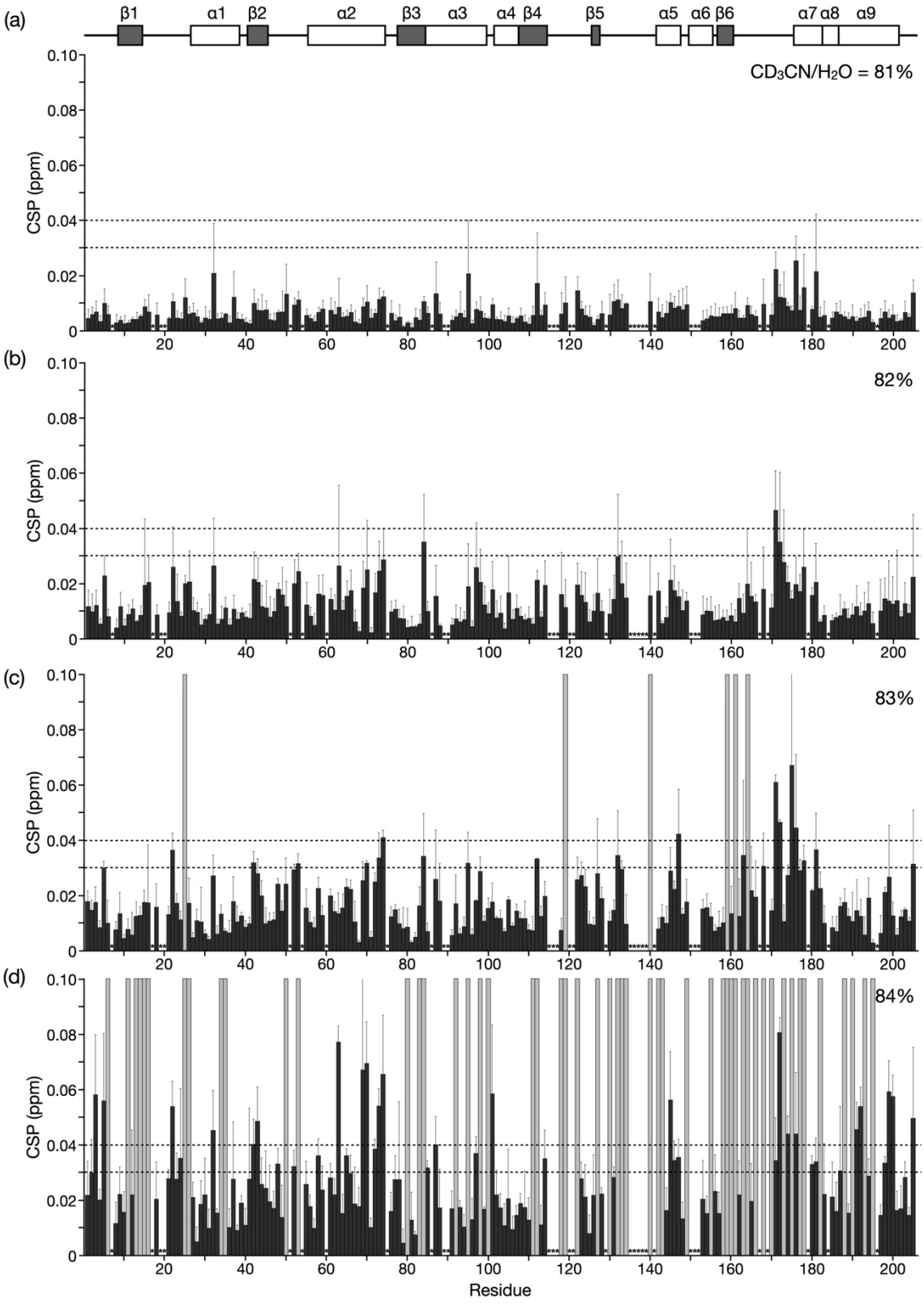

Figure S8 Chemical shift changes in the unfolding of CLE@1. CSP for each residue of caged CLE **1**, relative to 80% acetonitrile ratio. CD_3CN/H_2O = (a) 81%, (b) 82%, (c) 83%, (d) 84%. Error bars represent standard deviation. n = 3. Peaks that disappeared in each acetonitrile content are indicated by gray bars. The unassigned residues were denoted with asterisks.

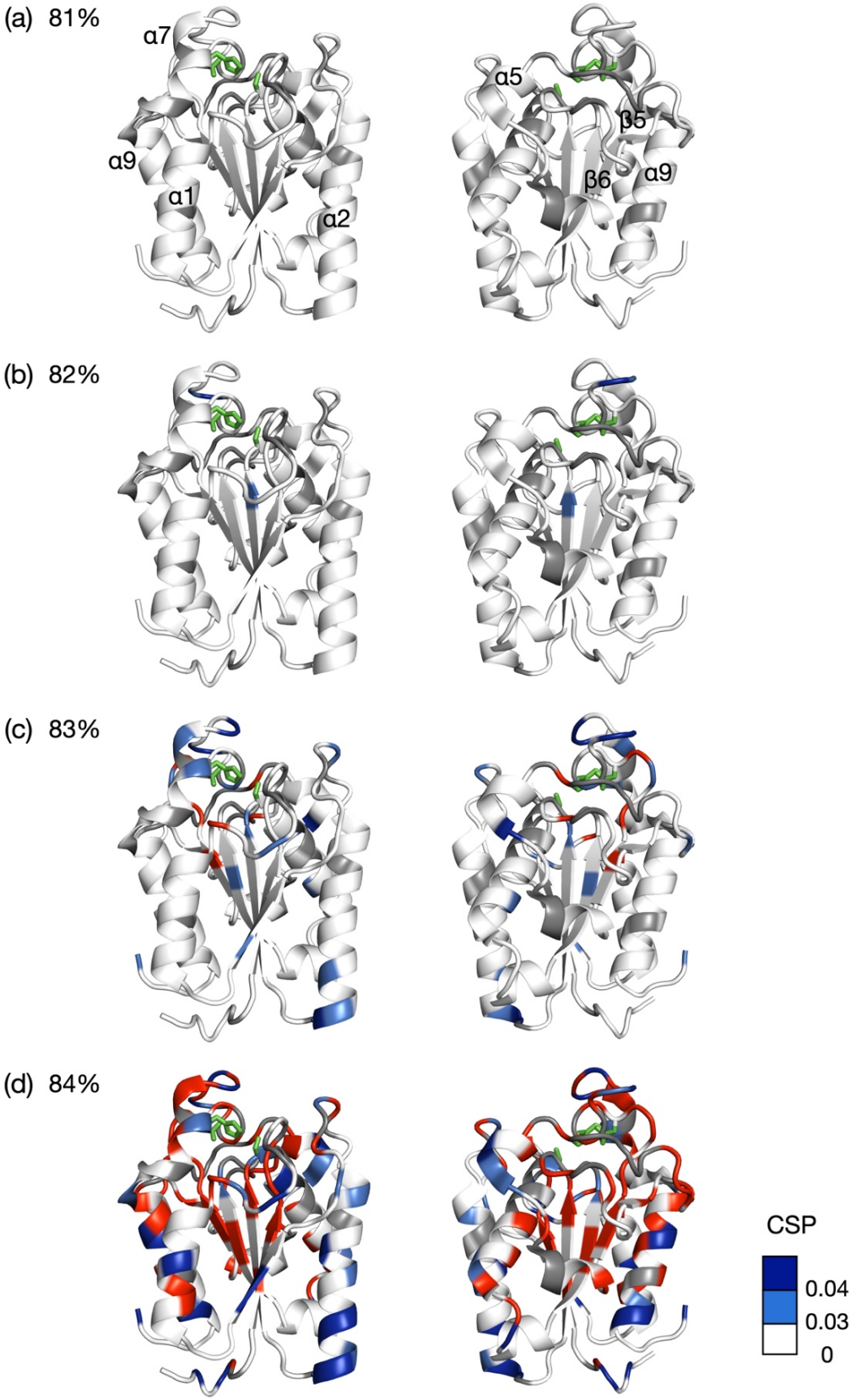

Figure S9 Mapping of CSP of CLE@1 unfolding. CSPs at each acetonitrile ratio were mapped on the CLE structure (PDB: 2CZQ), relative to 80%. CD_3CN/H_2O = (a) 81%, (b) 82%, (c) 83%, (d) 84%. The catalytic triad (S85, D165, and H180) is highlighted in green. The residues assigned to the disappeared peaks and unassigned residues are shown in red and gray, respectively. At 83% acetonitrile content, the α7 helix and some loops were perturbed, showing the structure change around the catalytic center.

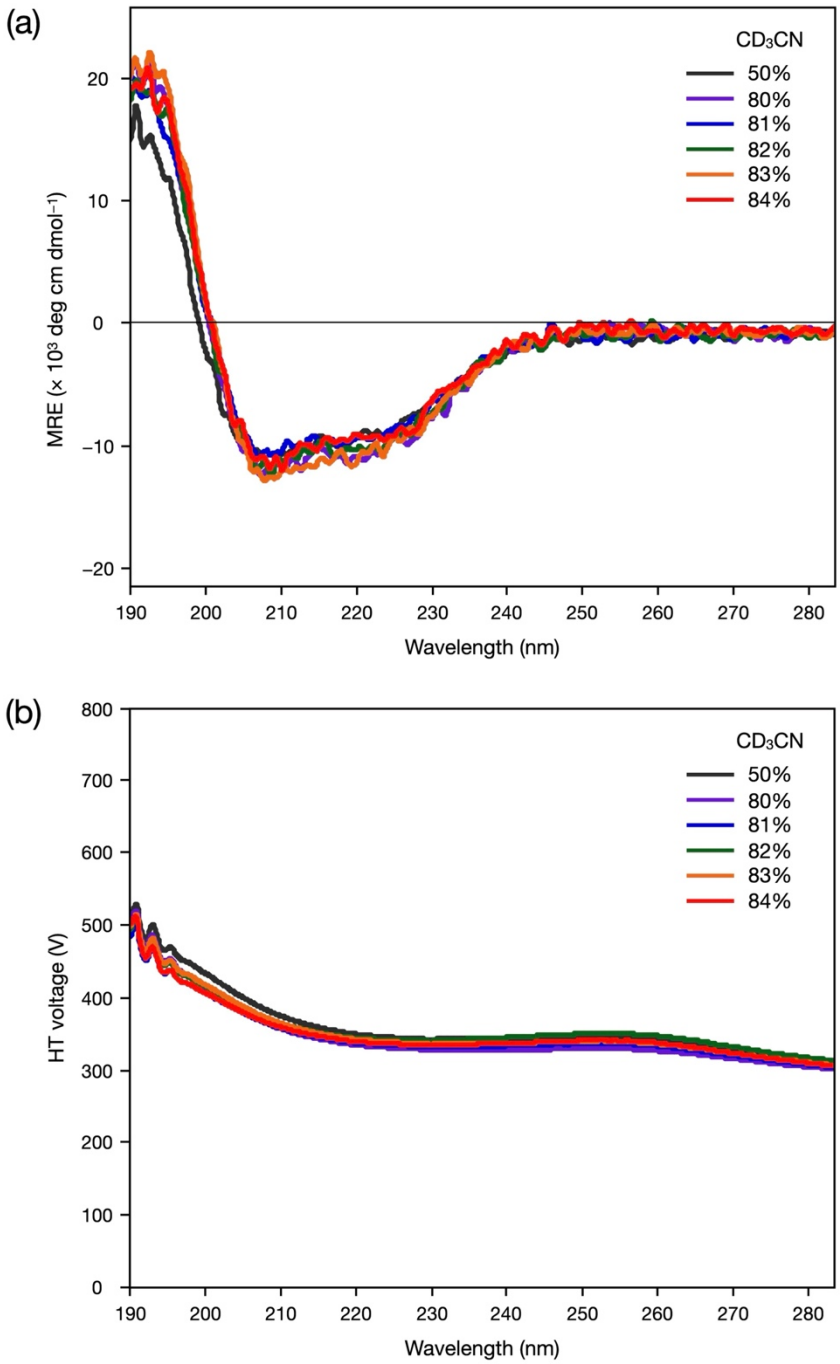

Figure S10 Circular dichroism (CD) spectra of CLE@1 in different acetonitrile/water mixtures. (a) Molar residue ellipticity (MRE) of CLE@**1**. (b) High tension (HT) voltage in each measurement. Even in over 82% acetonitrile, the spectra show little change, suggesting that caged CLE **1** partially unfolded into a molten globule that retains most of the secondary structure. HT voltages were within the range for reliable CD measurements (<700 V) although the large absorbance of acetonitrile and the cage resulted in fluctuations of the spectra at lower wavelength. 0.036 mg/mL CLE, number of scans: 8 (50%), 4 (80-84%).

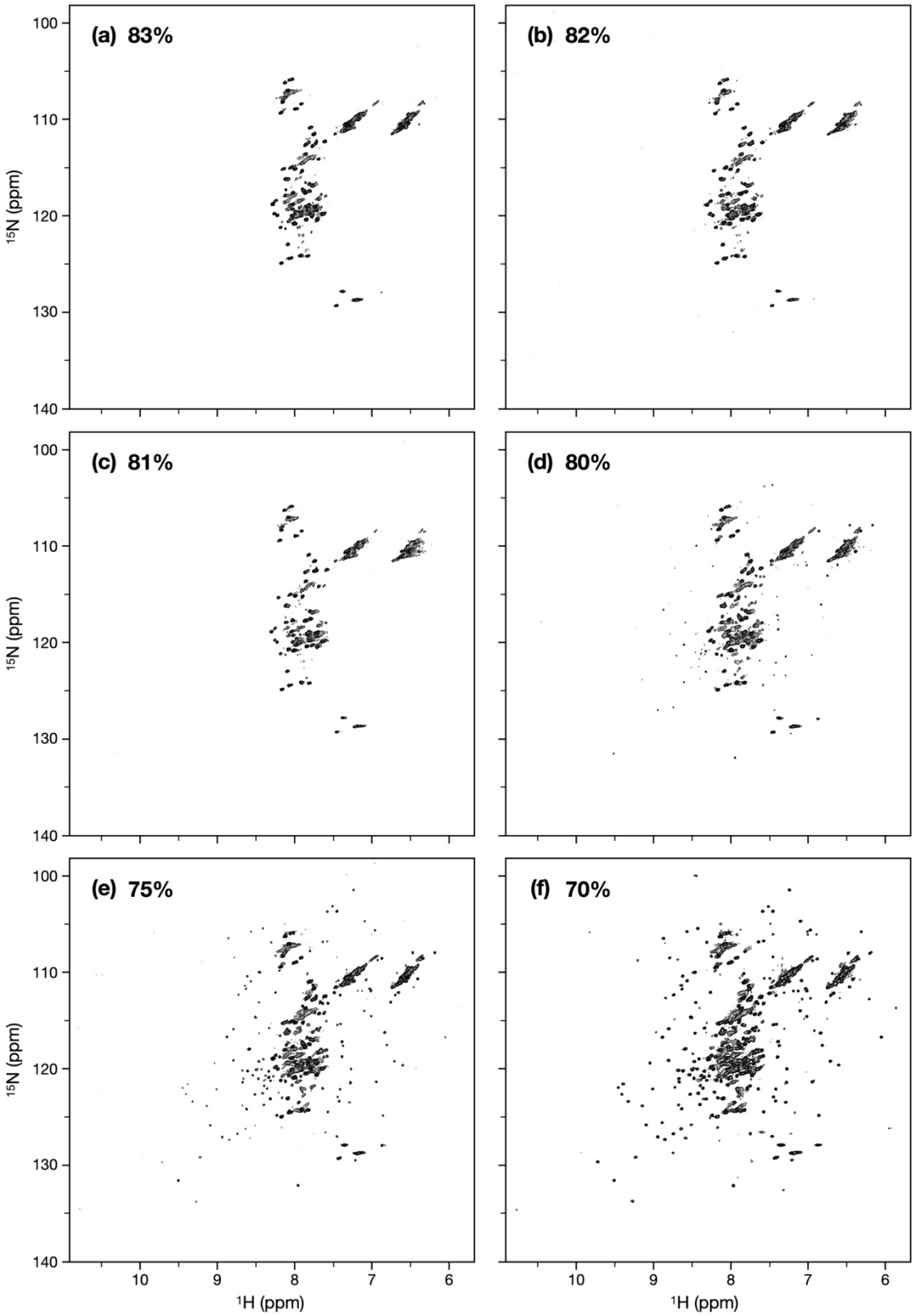

Figure S11 Refolding of CLE@1. ^{1}H–^{15}N HSQC spectra of the refolding of caged CLE **1** with decreasing acetonitrile content from 84% to 70% (800 MHz, 300 K). CD_3CN/H_2O = (a) 83:17, (b) 82:18 (c) 81:19 (d) 80:20, (e) 75:25, (f) 70:30. Although the caged CLE denatured at 83% acetonitrile, it started refolding below 80%. The folded structure was fully restored at 70%. Measurement time intervals (≥30 min) were long enough for the CLE folding (≤10^2 s: predicted from the protein length[5]). The spectra were identical when the intervals were extended.

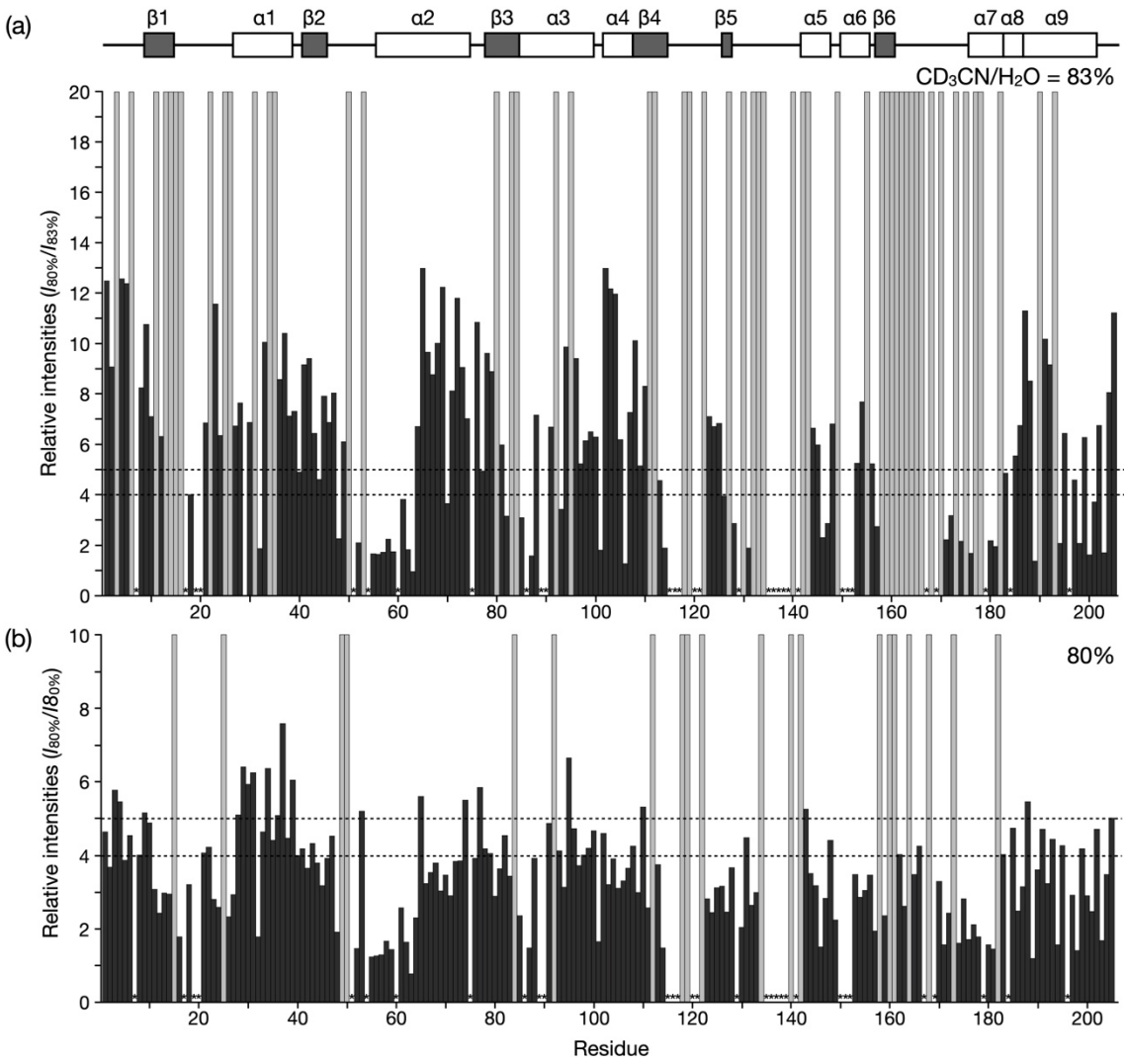
(a)
β1 α1 β2 α2 β3 α3 α4 β4 β5 α5 α6 β6 α7 α8 α9
CD3CN/H2O = 83%
Relative intensities (I80%/I83%)
(b)
80%
Relative intensities (I80%/I80%)
Residue

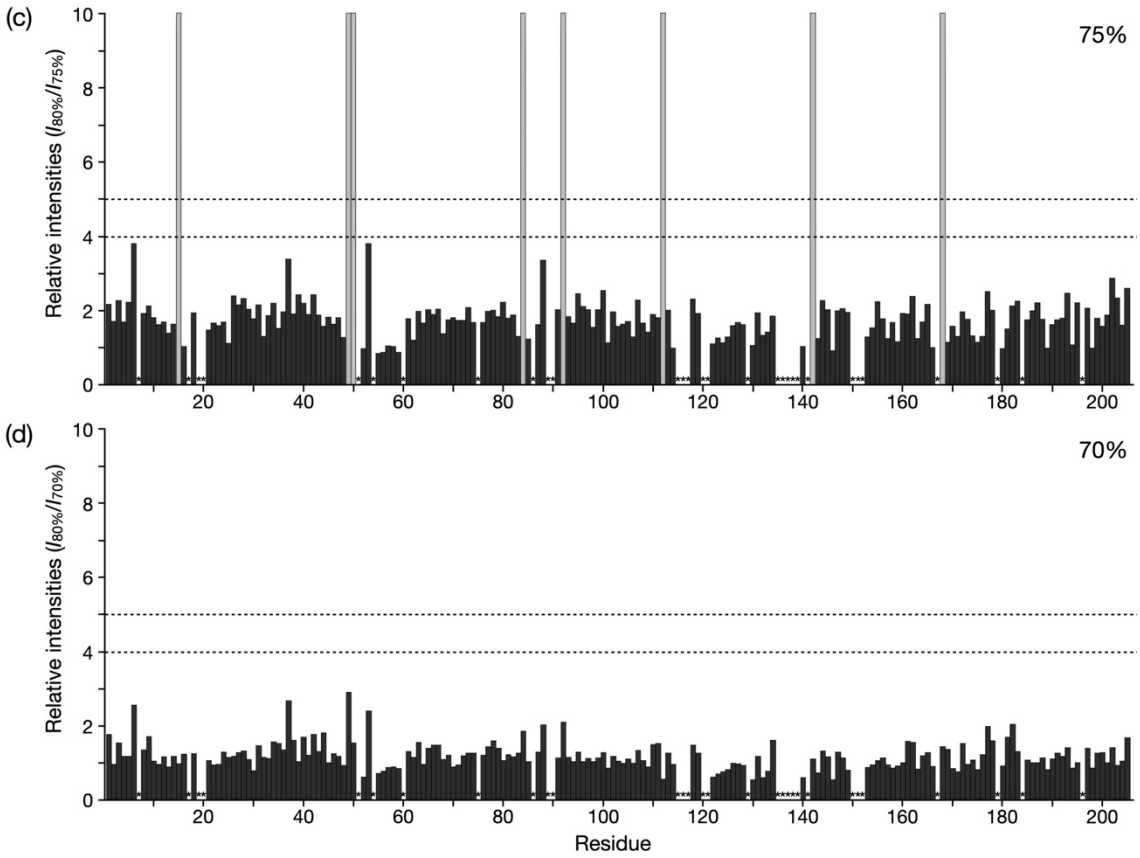

Figure S12 Cross-peak intensity recovery in the refolding of CLE@1. (a-d) Resonance intensities for each residue of caged CLE **1** relative to those at 80% acetonitrile ratio ($I_{80\%}$). CD_3CN/H_2O = (a) 83%, (b) 80%, (c) 75%, (d) 70%. The intensities were corrected taking into account dilution of the sample. Peaks that disappeared in each acetonitrile content are indicated by gray bars. The unassigned residues are denoted with asterisks. When caged CLE began refolding at 80%, some C-terminal domains (α5, α7), which collapsed first in the unfolding, were restored more than the other unfolded regions. This suggests that the refolding pathway might be different from that of the unfolding.

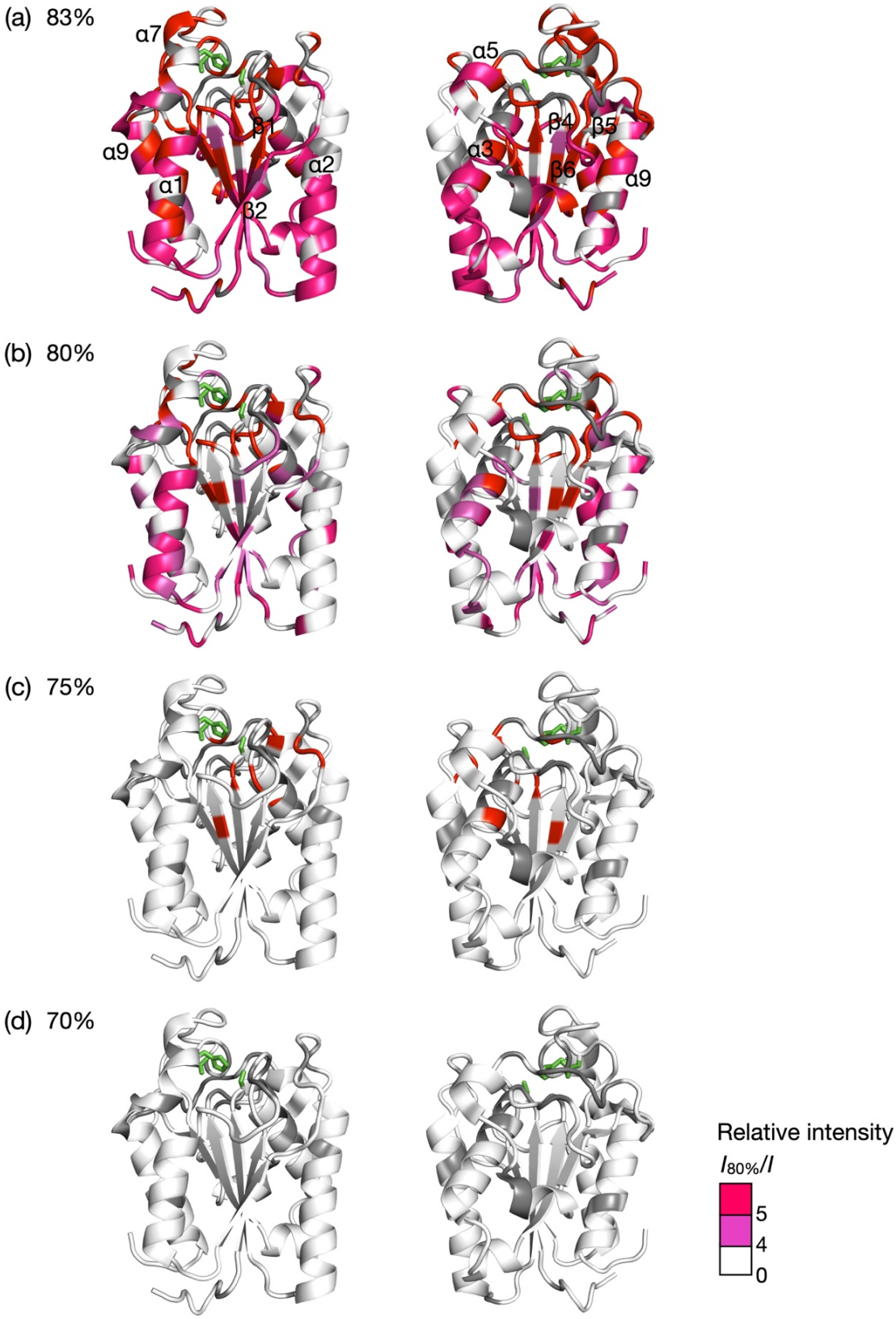

Figure S13 Mapping of the intensity recovery in the refolding of CLE@1. The relative intensities ($I_{80\%}/I$) were mapped on the CLE structure (PDB: 2CZQ). CD_3CN/H_2O = (a) 83%, (b) 80%, (c) 75%, (d) 70%. The catalytic triad (S85, D165, and H180) is highlighted in green. The residues assigned to the disappeared peaks and unassigned residues are shown in red and gray, respectively. The intensities were recovered not through the same pathway as the unfolding, suggesting that different pathways in the unfolding and refolding might have resulted in the hysteresis behavior of CLE.

Table S1 The acetonitrile-water ratio taking into account density changes in the titrant solutions.

$v_{ACN(app)}$ (v/v%)	$v_{ACN(actual)}$ in unfolding (v/v%)	$v_{ACN(actual)}$ in refolding (v/v%)
80.0	80.00	80.18
81.0	81.00	81.13
82.0	82.01	82.10
83.0	83.01	83.06
84.0	84.01	84.01

The apparent acetonitrile-water ratio, $v_{ACN(app)}$ (vol/vol%) is corrected into the actual ratio, $v_{ACN(actual)}$ (vol/vol%), by taking into account the different densities of the two titrant solutions and the resulting mixtures.[6] The systematic errors are shown to be negligible.

3. Synthesis of ligand 4

Instruments and Methods

^{1}H and ^{13}C NMR spectra were recorded on a Bruker AVANCE 500 MHz spectrometer equipped with a CP-TCI cryoprobe or a Bruker AVANCE III HD 500 MHz spectrometer equipped with a PABBO probe (500 MHz for ^{1}H NMR and 125 MHz for 13C NMR) at 300 K unless otherwise stated. TMS ($CDCl_3$ solution) in a capillary served as an internal standard (δ = 0 ppm for ^{1}H NMR), and solvent residual signals were used as a reference for the other cases ($CDCl_3$: 77.16 ppm for ^{13}C, DMSO-d_6: δ 2.50 ppm for ^{1}H and 39.52 ppm for ^{13}C, CD_3CN: δ 1.94 ppm for ^{1}H). High-resolution electrospray ionization mass spectrometry (ESI-HRMS) was performed on a Waters Xevo G2-XS QTof. Gel permeation chromatography was performed on a LC-9260 II equipped with JAIGEL-2HR-40 (Japan Analysis Industry Co., Ltd.) as a column. High performance liquid chromatography (HPLC) was performed using JASCO EXTREMA System using Inertsil ODS-3 (GL Sciences) as a column.

Solvents and reagents were purchased from TCI Co., Ltd., FUJIFILM Wako Pure Chemical Corp., Sigma-Aldrich Co., and Kanto Chemical Co., Inc. and used without further purification. Silica Gel 60 N (neutral, particle size 40-100 μm, Kanto Chemical Co., Inc.) and YMC*GEL ODS-A (particle size 150 μm, YMC. Co., Ltd.) were used for normal-phase and reversed-phase column chromatography, respectively.

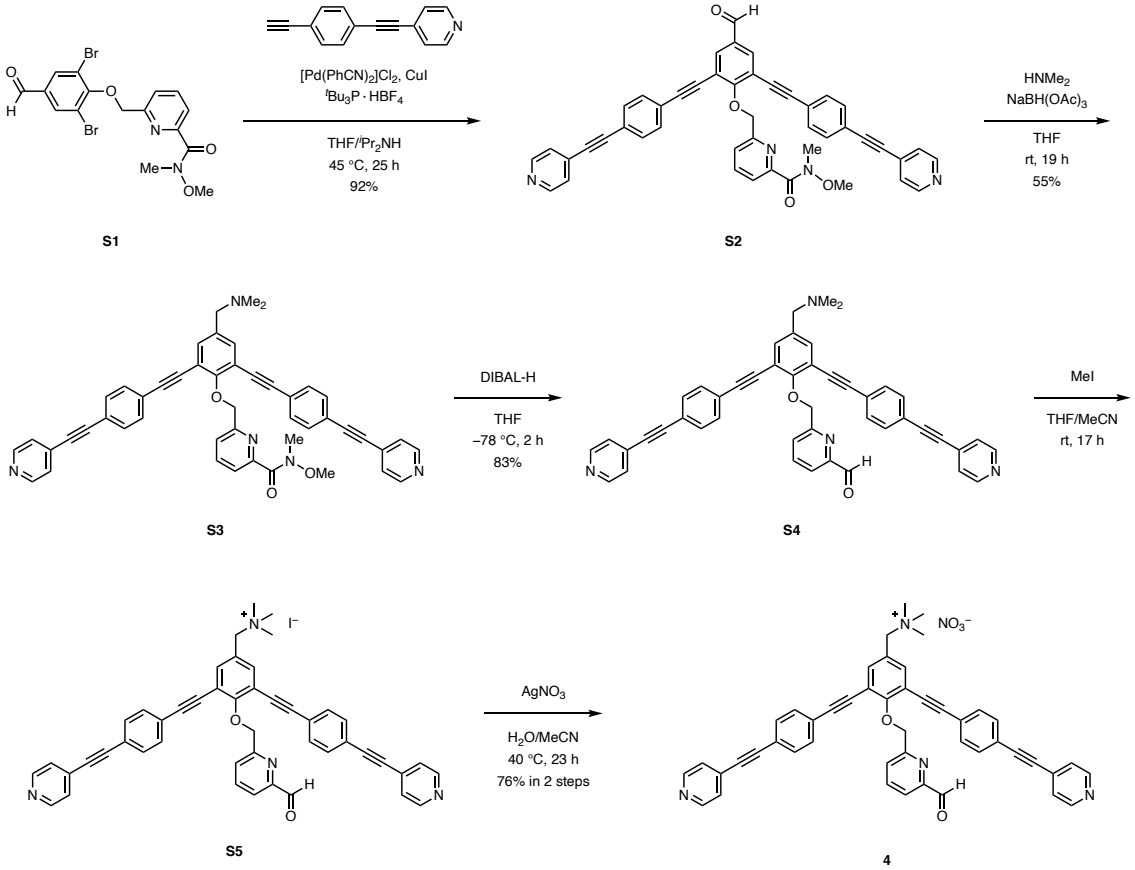

Scheme S1 Synthesis of ligand 4

Synthesis of 6-((4-formyl-2,6-bis((4-(pyridine-4-ylethynyl)phenyl)ethynyl)phenoxy)methyl)-*N*-methoxy-*N*-methylpicolinamide (**S2**)

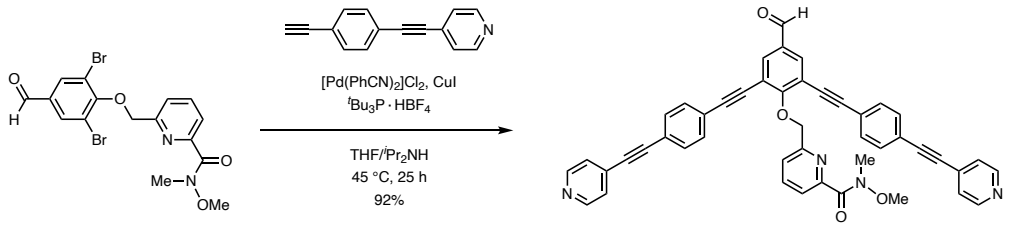

S1 **S2**

A mixture of 6-((2,6-dibromo-4-formylphenoxy)methyl)-*N*-methoxy-*N*-methylpicolin-amide (**S1**, 314 mg, 0.69 mmol), bis(benzonitrile)palladium(II) dichloride (36.2 mg, 0.094 mmol), tri(*tert*-butyl)phosphine tetrafluoroborate (55.3 mg, 0.19 mmol), CuI (36.0 mg, 0.19 mmol), and diisopropylamine (1.1 mL) in dry THF (30 mL) was degassed by three freeze-pump-thaw cycles. To the mixture was added 4-(4-ethynylphenyl)pyridine (344 mg, 1.69 mmol) in two portions, and the resulting suspension was stirred at 45 °C for 22 h under argon atmosphere. As incompletion of the reaction was suggested by TLC, to the mixture were added bis(benzonitrile)palladium(II) dichloride (22.8 mg, 0.060 mmol) and 4-(4-etynylphenyl)-ethynyl)pyridine (115 mg, 0.57 mmol). After stirring at 45 °C for 3 h, the resulting suspension was mixed with $CHCl_3$ (14 mL) and water (3 mL) and filtered through celite pad. The aqueous layer was separated and extracted with $CHCl_3$ (7 mL × 6). The combined organic layer was washed with brine (7 mL), dried over Na_2SO_4. The solvent was evaporated in vacuo, and the residue was purified by silica gel column chromatography ($CHCl_3$/MeOH = 97:3 and then $CHCl_3$/EtOAc/MeOH = 60:40:3) to give 6-((4-formyl-2,6-bis((4-(pyridine- 4-ylethynyl)phenyl)-ethynyl)phenoxy)methyl)-*N*-methoxy-*N*-methylpicolinamide (**S2**) as a pale yellow powder (442 mg, 0.629 mmol, 92% yield).

HRMS (ESI) m/z: $[M+H]^+$: calcd for $C_{46}H_{31}N_4O_4$ 703.2345, found 703.2338;
^{1}H NMR (500MHz, $CDCl_3$, 300 K) δ 9.95 (s, 1H), 8.63 (d, *J* = 5.8 Hz, 4H), 8.04 (s, 2H), 8.00 (d, *J* = 7.9 Hz, 1H), 7.81 (dd, *J* = 7.9, 7.9 Hz, 1H), 7.59 (br, 1H), 7.53 (d, *J* = 8.3 Hz, 4H), 7.44 (d, *J* = 8.3 Hz, 4H), 7.40 (d, *J* = 5.8 Hz, 4H), 5.71 (s, 2H), 3.66 (br, 3H), 3.37 (s, 3H);
^{13}C NMR (125 MHz, $CDCl_3$, 300 K) δ 189.5, 169.1 (br), 164.5, 156.1, 152.7, 149.9, 137.5, 135.1, 132.2, 132.0, 131.7, 131.1, 125.6, 123.2, 122.8 (br), 122.7, 122.3 (br), 117.9, 95.2, 93.3, 88.9, 86.4, 75.9, 61.5, 33.0 (br).

Synthesis of 6-((4-((dimethylamino)methyl)-2,6-bis((4-(pyridine-4-ylethynyl)phenyl)ethynyl)-phenoxy)methyl)-*N*-methoxy-*N*-methylpicolinamide (**S3**)

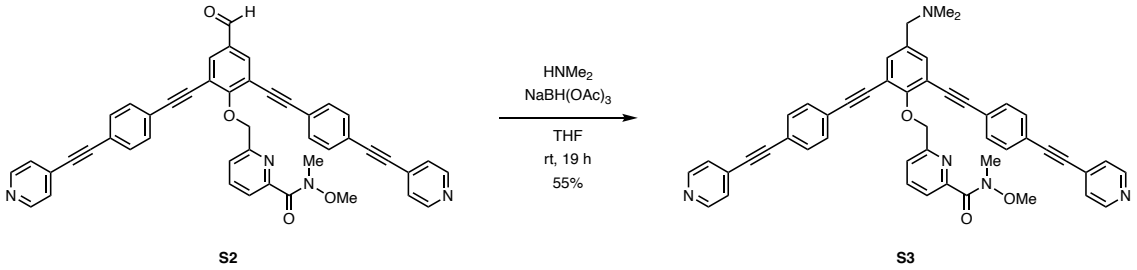

S2 **S3**

To a solution of compound **S2** (442 mg, 0.629 mmol) and dimethylamine (4.6 mL, ca. 2 M in THF) in dry THF (30 mL) was added sodium tri(acetoxy)borohydride (1.01 g, 4.79 mmol) at 0 °C in 2 portions. The resulting suspension was stirred at room temperature for 19 h under argon atmosphere. Water (18 mL) and CH_2Cl_2 (18 mL) were sequentially added to the mixture, and the aqueous layer was separated and extracted with CH_2Cl_2 (18 mL × 4). The combined organic layer was washed with brine (18 mL) and dried over Na_2SO_4. The solvent was evaporated in vacuo, and the residue was purified by silica gel column chromatography ($CHCl_3$/MeOH = 94:6) and GPC ($CHCl_3$). The obtained crude product was dissolved in $CHCl_3$ and reprecipitated with Et_2O to give 6-((4-((dimethylamino)methyl)-2,6-bis((4-(pyridine-4-ylethynyl)-phenyl)ethynyl)phenoxy)methyl)-*N*-methoxy-*N*-methylpicolinamide (**S3**) (254 mg, 0.347 mmol, 55% yield) give as a pale-yellow solid.

HRMS (ESI) m/z: $[M+H]^+$: calcd for $C_{48}H_{38}N_5O_3$ 732.2975, found 732.2982;
^{1}H NMR (500MHz, $CDCl_3$, 300 K) δ 8.62 (d, *J* = 6.0 Hz, 4H), 8.02 (d, *J* = 7.9 Hz, 1H), 7.78 (dd, *J* = 7.8, 7.8 Hz, 1H), 7.58 (br, 1H), 7.53 (s, 2H), 7.51 (d, *J* = 7.8 Hz, 4H), 7.49 (d, *J* = 7.8 Hz, 4 H), 7.38 (d, *J* = 6.0 Hz, 4H), 5.55 (s, 2H), 3.69 (br, 3H), 3.42 (s, 2H), 3.36 (s, 3H), 2.30 (s, 6H);
^{13}C NMR (125 MHz, $CDCl_3$, 288 K) δ 169.8, 159.7, 157.0, 152.6, 149.9, 137.5, 134.9, 134.5, 132.0, 131.6, 131.2, 125.6, 123.8, 123.0, 122.2, 121.8, 117.3, 93.8, 93.5, 88.6, 87.6, 76.0, 63.1, 61.7, 45.4, 32.8.

Synthesis of 6-((4-((Dimethylamino)methyl)-2,6-bis((4-(pyridine-4-ylethynyl)phenyl)ethynyl)-pheolxy)methyl)picolinaldehyde (**S4**)

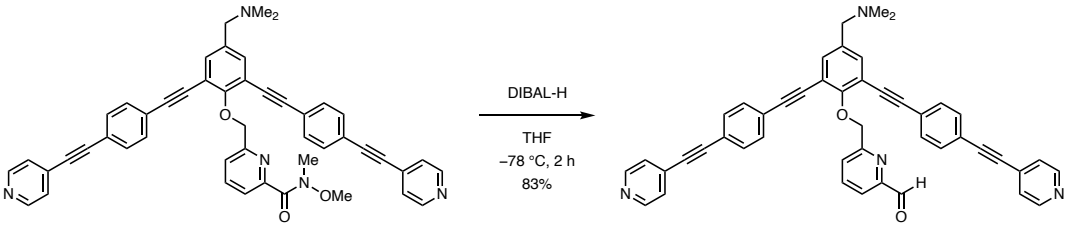

S3 **S4**

To a solution of compound **S3** (320 mg, 0.44 mmol) in dry THF (70 mL) was added diisobutylaluminium hydride (2.3 mL, ca. 1 M in hexane) dropwise at −78 °C. The resulting mixture was stirred at −78 °C for 2 h under argon atmosphere, and the reaction was quenched by the successive addition of MeOH (2.3 mL) and ethyl acetate (4.6 mL). After warming to room temperature, to the mixture were added saturated aqueous Rochelle salt (12 mL). The aqueous layer was separated and extracted with ethyl acetate (12 mL × 4). The organic layer was washed with saturated Rochelle salt (12 mL) and brine (12 mL). The aqueous layer was extracted again with ethyl acetate (24 mL × 3). The combined organic layer was dried over Na_2SO_4, and the solvent was evaporated in vacuo. The residue was purified by silica gel column chromatography ($CHCl_3$/MeOH = 96:4). The obtained yellow oil was dissolved in 1,4-dioxane and lyophilized to give 6-((4-((dimethylamino)methyl)-2,6-bis((4-(pyridine-4-ylethynyl)-phenyl)ethynyl)pheolxy)methyl)-picolinaldehyde (**16**) as a yellow powder (243 mg, 0.36 mmol, 83% yield).

HRMS (ESI) m/z: $[M+H]^+$: calcd for $C_{46}H_{33}N_4O_2$ 673.2604, found 673.2599;
^{1}H NMR (500MHz, $CDCl_3$, 300 K) δ 10.04 (s, 1H), 8.62 (d, *J* = 5.7 Hz, 4H), 8.16 (d, *J* = 7.5 Hz, 1H), 7.89 (dd, *J* = 7.5, 7.5 Hz ,1H), 7.85 (d, *J* = 7.5 Hz, 1H), 7.52 (s, 2H), 7.50 (d. *J* = 8.2 Hz, 4H), 7.42 (d, *J* = 8.2 Hz, 4H), 7.38 (d, *J* = 5.8 Hz, 4H), 5.60 (s, 2H), 3.41 (s, 2H), 2.30 (s, 6H);
^{13}C NMR (125 MHz, $CDCl_3$, 288 K) δ 193.5, 159.5, 158.8, 152.1, 150.0, 137.8, 135.4, 134.5, 132.0, 131.6, 131.2, 126.4, 125.6, 123.8, 122.3, 120.9, 117.3, 93.8, 93.5, 88.7, 87.6, 75.9, 63.2, 45.6.

Synthesis of 1-((4-((6-Formylpyridin-2-yl)methoxy)-3,5-bis((4-(pyridine-4-ylethynyl)phenyl)-ethynyl)phenyl)-*N*,*N*,*N*-trimethyl)methylammonium nitrate (**4**)

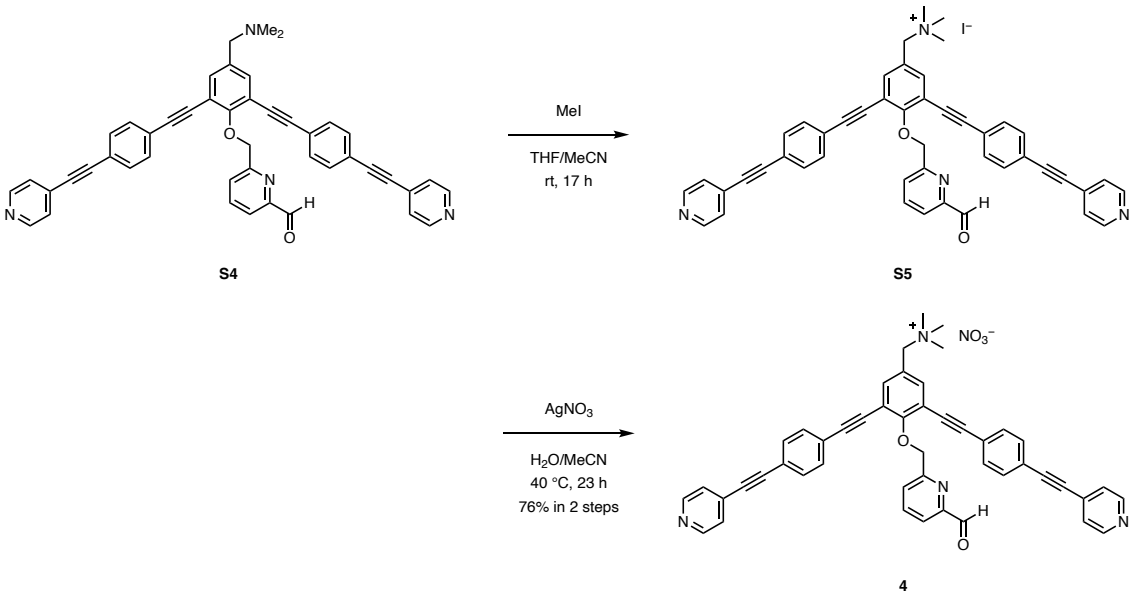

To a suspension of compound **S4** (157 mg, 0.234 mmol) in dry THF (0.7 mL) and dry acetonitrile (3.4 mL) was added 0.48% methyl iodide solution (THF/MeCN=1:5, (v/v), 3.0 mL, 0.23 mmol) at 0 °C. The resulting suspension was stirred at room temperature for 17 h under argon atmosphere. The solvent was evaporated in vacuo to give 1-((4-((6-formylpyridin-2-yl)methoxy)-3,5-bis((4-(pyridine-4-ylethynyl)phenyl)ethynyl)phenyl)-*N*,*N*,*N*-trimethyl)methyl-ammonium iodide (**S5**) as a bright yellow powder (173 mg,). The product was used in the following reaction without further purification.

To a suspension of compound **S5** (173 mg) in acetonitrile (1.4 mL) and water (13 mL) was added silver nitrate (38.8 mg, 0.23 mmol). The resulting mixture was stirred at 40 °C for 23 h and filtered through celite pad. The solvent was evaporated in vacuo and the pale-yellow residue was purified by reversed-phase silica gel column chromatography (H_2O/MeCN = 7:3-0:10). The obtained crude was dissolved in water and acetonitrile, and the solvent was slowly evaporated to yield 1-((4-((6-formylpyridin-2-yl)methoxy)-3,5-bis((4-(pyridine-4-ylethynyl)phenyl)ethynyl)phenyl)-*N*,*N*,*N*-trimethyl)methylammonium nitrate (**4**) as a pale yellow powder (134 mg, 0.179 mmol, 76% yield in 2 steps).

Compound **S5**

HRMS (ESI) m/z: $[M-I]^+$: calcd for $C_{47}H_{35}N_4O_2$ 687.2755, found: 687.2745;

^{1}H NMR (500MHz, DMSO-d_6, 300 K) δ 9.94 (s, 1H), 8.66 (d, J = 6.7 Hz, 4H), 8.10 (d, J = 7.7 Hz, 1H), 8.06 (dd, J = 7.7, 7.7 Hz, 1H), 7.91 (d, J = 7.7 Hz, 1H), 7.86 (s, 2H), 7.68 (d, J = 8.5 Hz, 4H), 7.57 (d, J = 8.5 Hz, 4H), 7.55 (d, J = 6.7 Hz, 4H), 5.66 (s, 2H), 4.53 (s, 2H), 4.09 (s, 9H);

Ligand **4**

HRMS (ESI) m/z: $[M-NO_3]^+$: calcd for $C_{47}H_{35}N_4O_2$ 687.2755, found: 687.2745;

HPLC: t_R =35.45 min (20-50% linear gradient of MeCN in 0.1% TFA aq., 30 °C);

m.p.: 135 °C (decomposed);

^{1}H NMR (500MHz, DMSO-d_6, 300 K) δ 9.94 (s, 1H), 8.66 (d, J = 5.2 Hz, 4H), 8.11 (d, J = 7.5 Hz, 1H), 8.07 (dd, J = 7.5, 7.5 Hz, 1H), 7.91 (d, J = 7.1 Hz, 1H), 7.87 (s, 2H), 7.68 (d, J = 8.2 Hz, 4H), 7.57 (d, J = 8.2 Hz, 4H), 7.55 (d, J = 5.2 Hz, 4H), 5.66 (s, 2H), 4.55 (s, 2H), 3.10 (s, 9H);

^{13}C NMR (125 MHz, DMSO-d_6, 300 K) δ 193.2, 161.2, 157.2, 151.8, 150.0, 138.6, 138.2, 132.2, 131.7, 129.9, 126.9, 125.4, 124.9, 122.7, 121.9, 121.5, 117.1, 94.2, 92.8, 88.8, 86.9, 75.9, 66.4, 52.0.

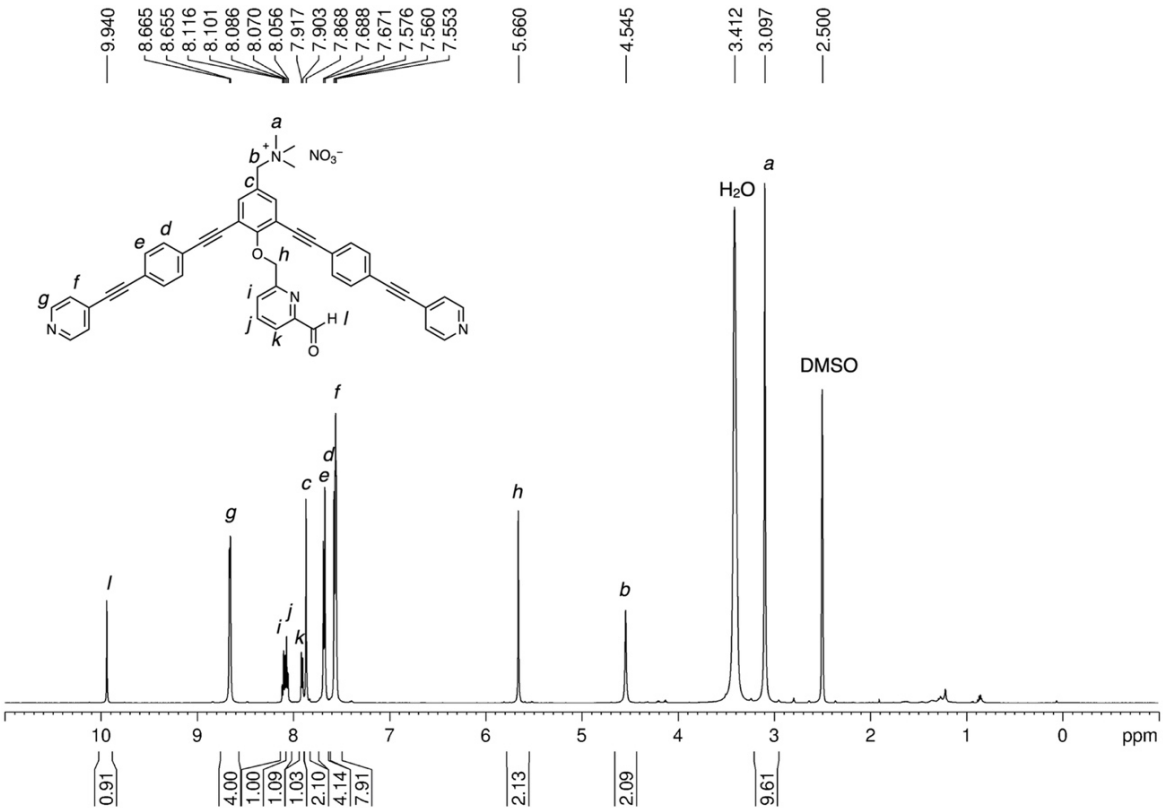

Figure S14 ^{1}H NMR spectrum of ligand 4 (500 MHz, DMSO-d_6, 300 K).

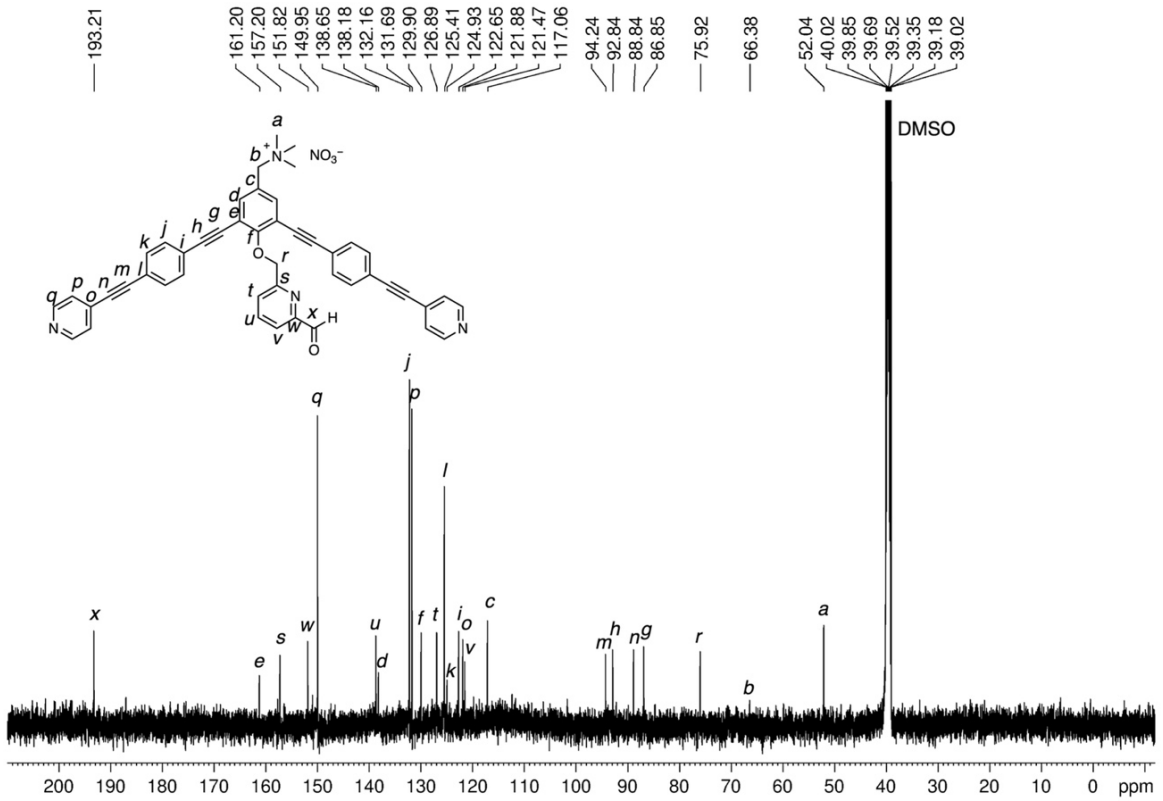

Figure S15 ^{13}C NMR spectrum of ligand 4 (125 MHz, DMSO-d_6, 300 K).

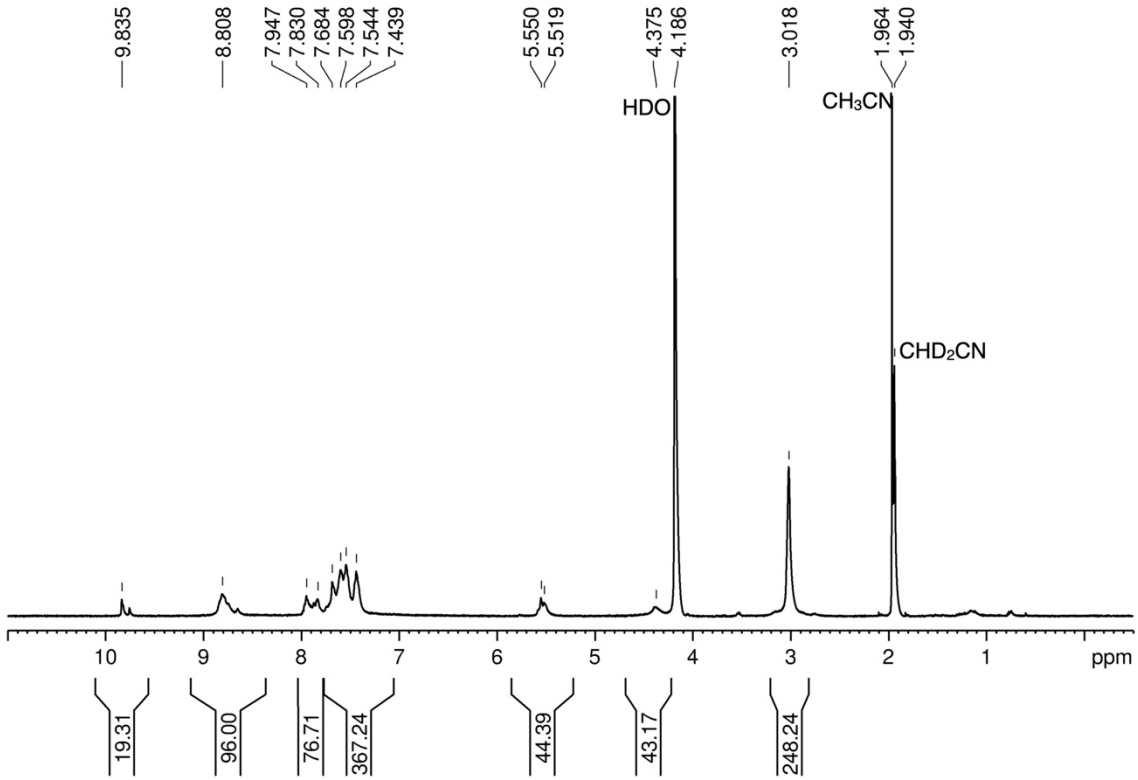

Figure S16 ^{1}H NMR spectrum of complex 2 (500 MHz, CD_3CN/D_2O = 1:1, 300 K). Cage **2** was self-assembled from ligand **4** with $[Pd(MeCN)_4](BF_4)_2$.

4. Preparation and characterization of caged CLE 2 (CLE@2)

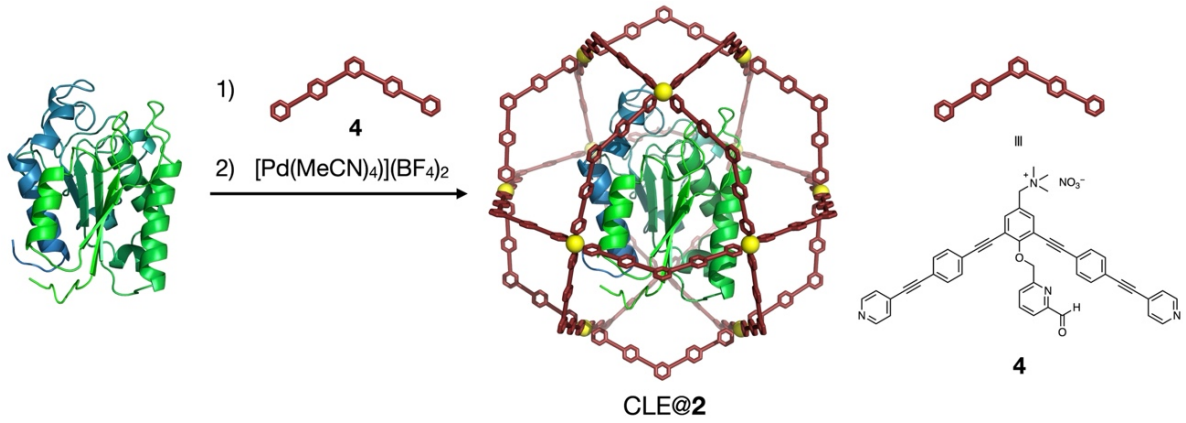

Scheme S2 Preparation of CLE@2. The protein is first conjugated to ligand **4** via N-terminus specific condensation with 2-formylpyridine.[2,7] The successive self-assembly with Pd(II) ions affords an $M_{12}L_{24}$ complex that encapsulates CLE in a one-pot manner. See Materials and Methods for detail.

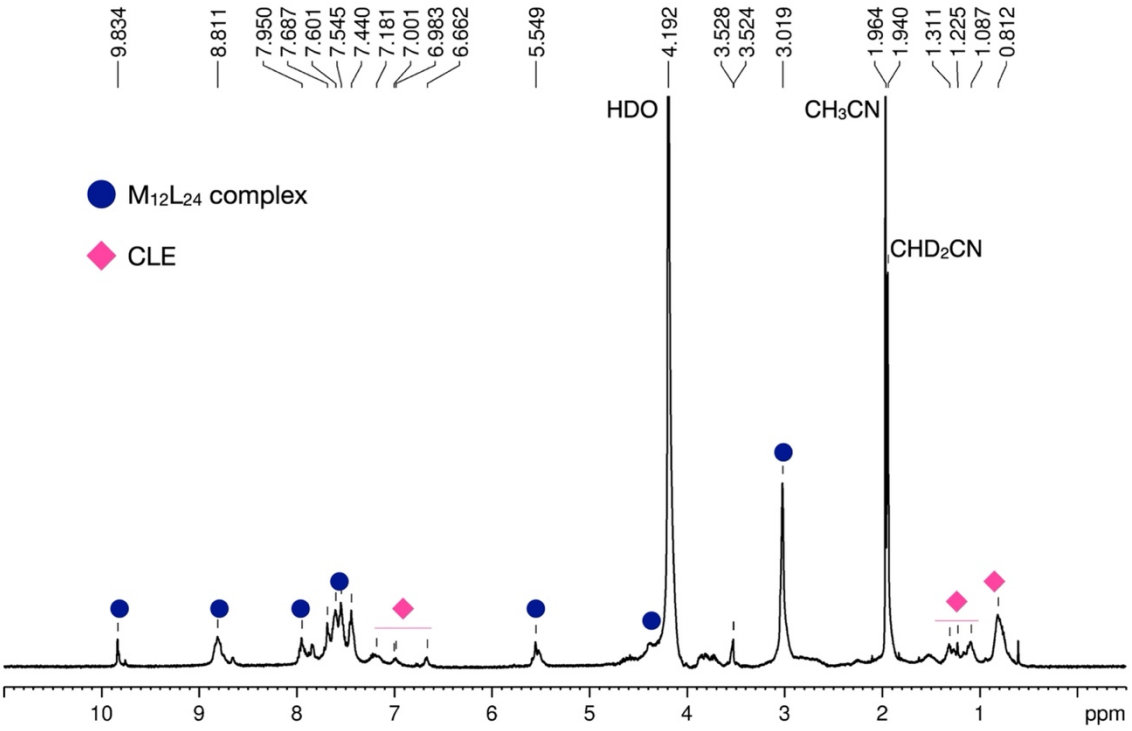

Figure S17 ^{1}H NMR spectrum of CLE@2 (500 MHz, CD_3CN/D_2O = 1:1, 300 K).

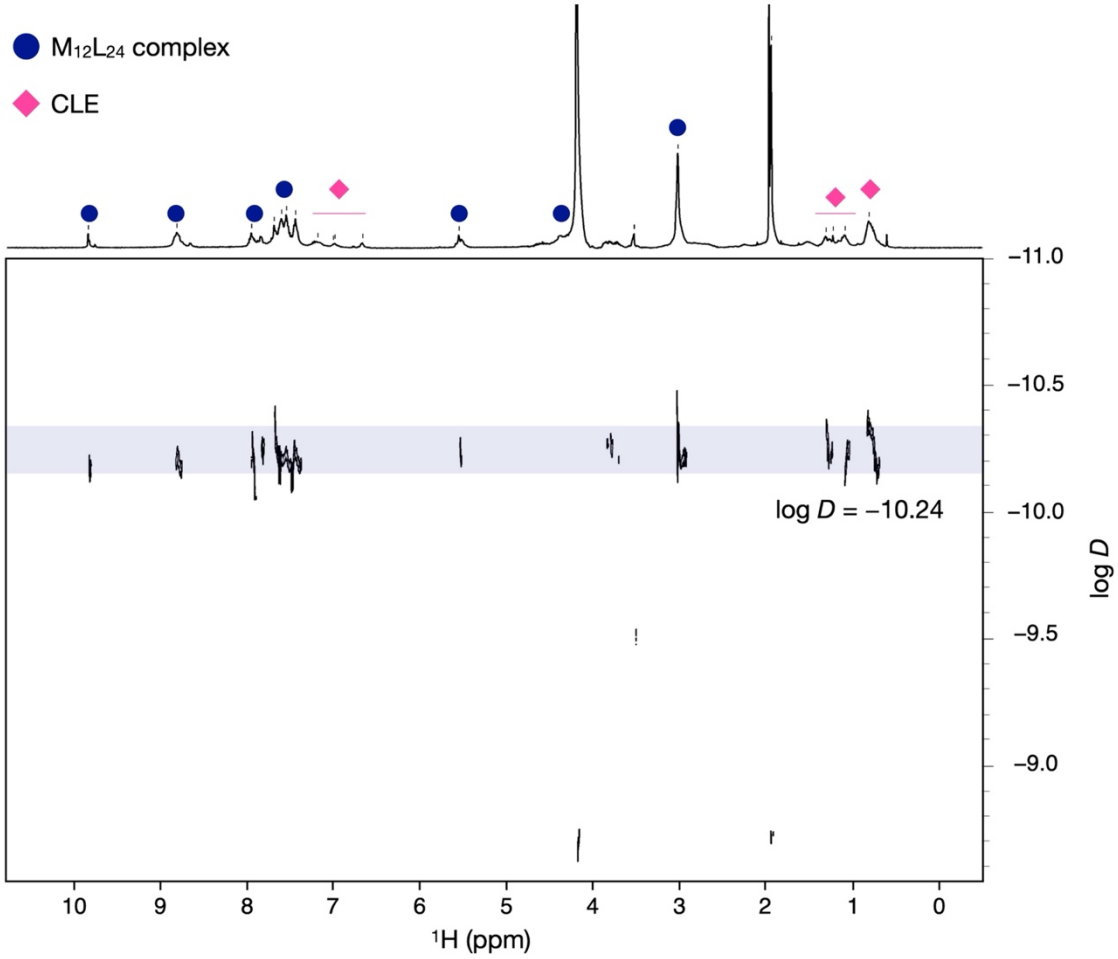

Figure S18 ^{1}H DOSY NMR spectrum of CLE@2 (500 MHz, CD_3CN/D_2O = 1:1, 300 K). Upon encapsulation in the cage, the diffusion coefficient *D* of CLE was decreased from 1.3 $\times10^{-10}$ m^2/s (log *D* = −9.88) to 5.8 $\times10^{-11}$ m^2/s (log *D* = −10.24). The value of caged CLE@**2** was identical to that of complex **2**. These results demonstrate that CLE was confined in the coordination sphere. Notably, the *D* value of CLE@**2** was also smaller than CLE@**1** (7.2 $\times10^{-11}$ m^2/s, log *D* = −10.14),[2,8] indicating the encapsulation in a larger cage.

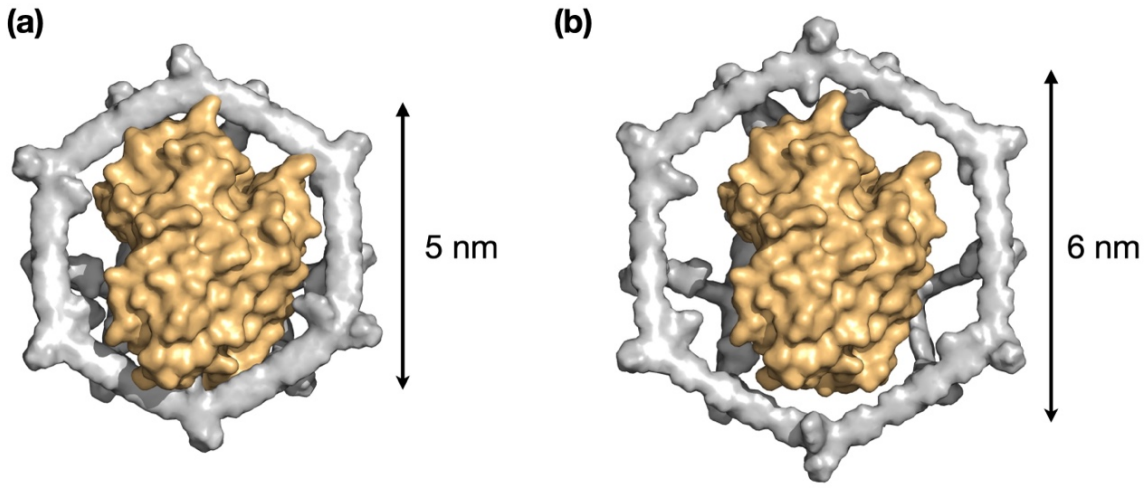

Figure S19 Molecular modeling of CLE in $M_{12}L_{24}$ cages. (a) CLE@**1** and (b) CLE@**2**. The solvent-accessible surface areas of the $M_{12}L_{24}$ complexes and CLE are shown in silver and pale orange, respectively. The inner diameters of complexes **1** and **2** were estimated to be around 5 nm and 6 nm, respectively (cf. maximum diameter of CLE: ~4.5 nm). CLE@**2** has some free inner space although CLE@**1** is tightly packed in the cage.

5. Unfolding/refolding of CLE@2

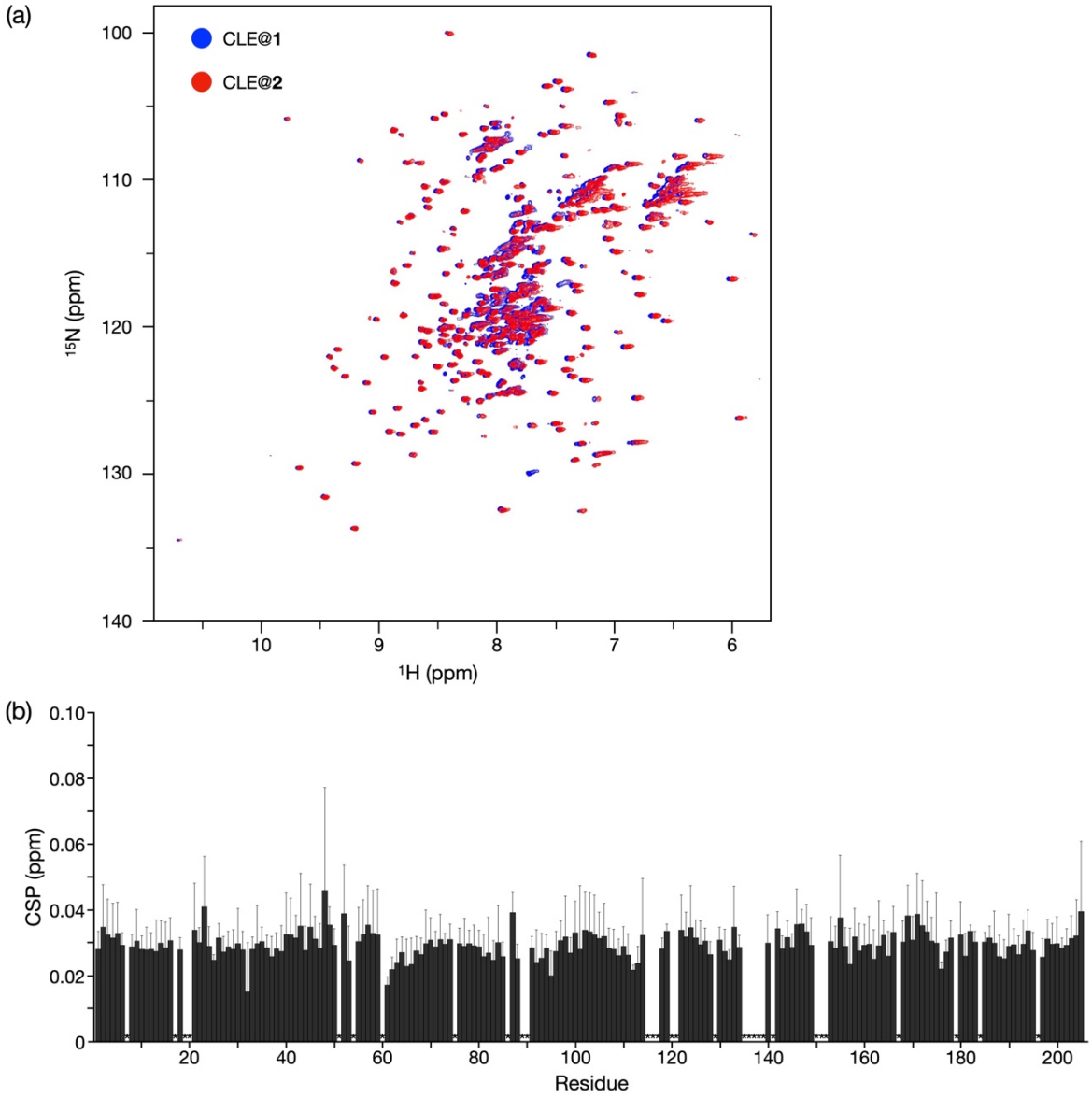

Figure S20 Comparison of CLE@2 with CLE@1. (a) The overlay of ^{1}H–^{15}N HSQC NMR spectra of caged CLE **1** (blue) and **2** (red) (800 MHz, CD_3CN/H_2O = 1:1, 300 K). Almost all the cross-peaks are overlapped, showing CLE@**2** has the same native structure as CLE@**1**. (b) CSP for each residue of caged CLE **2** at 80% acetonitrile, compared with CLE@**1**. Error bars represent standard deviation. n = 3. The small CSPs were attributed to the sample variations.

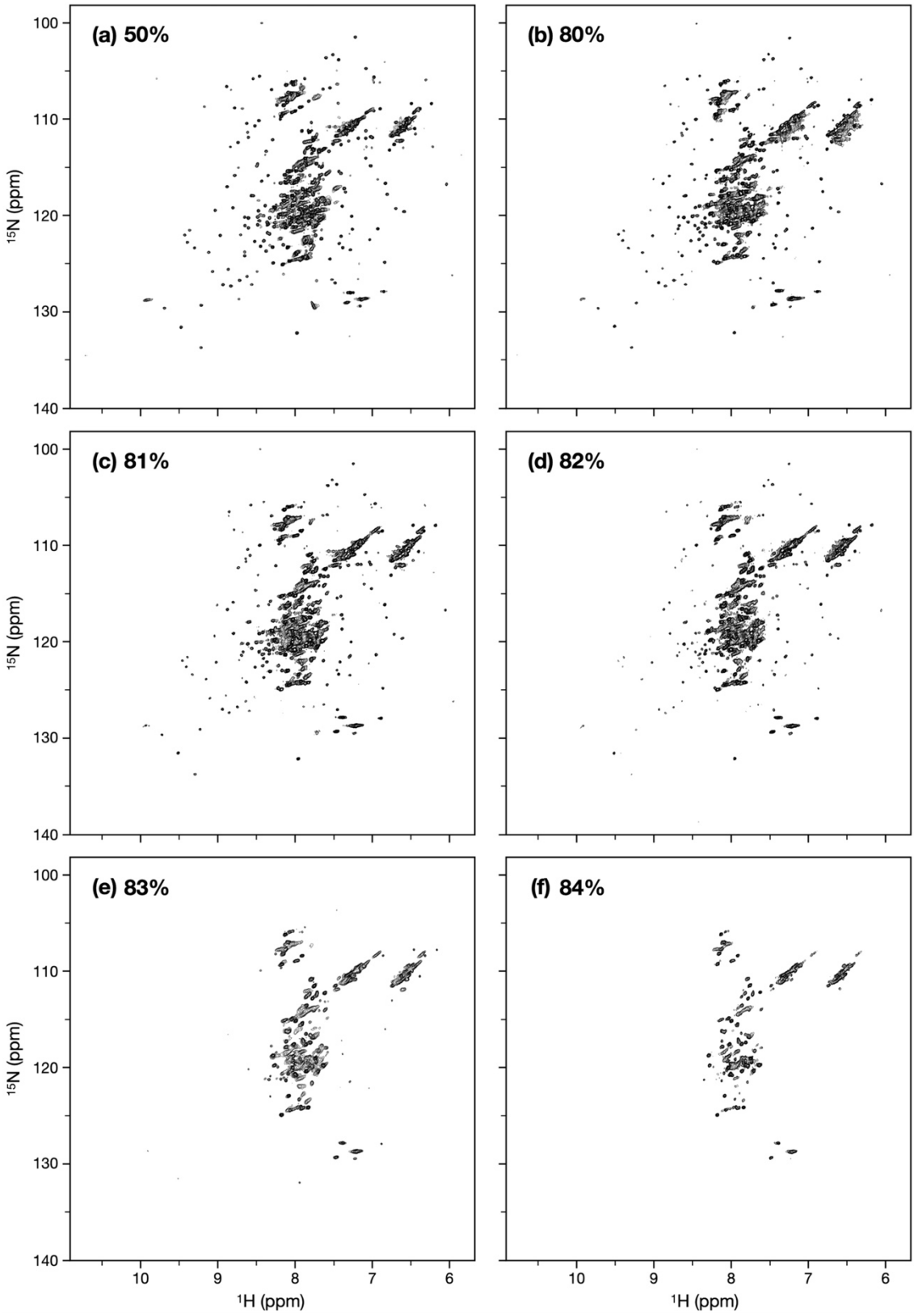

Figure S21 Unfolding of CLE@2. ^{1}H–^{15}N HSQC spectra of unfolding of caged CLE **2** with increasing the acetonitrile ratio (800 MHz, 300 K). CD_3CN/H_2O = (a) 50:50, (b) 80:20, (c) 81:19, (d) 82: 18, (e) 83:17, (f) 84:16. Similar to CLE@**1**, CLE in complex **2** collapsed at 83% acetonitrile, and the unfolding was completed at 84%.

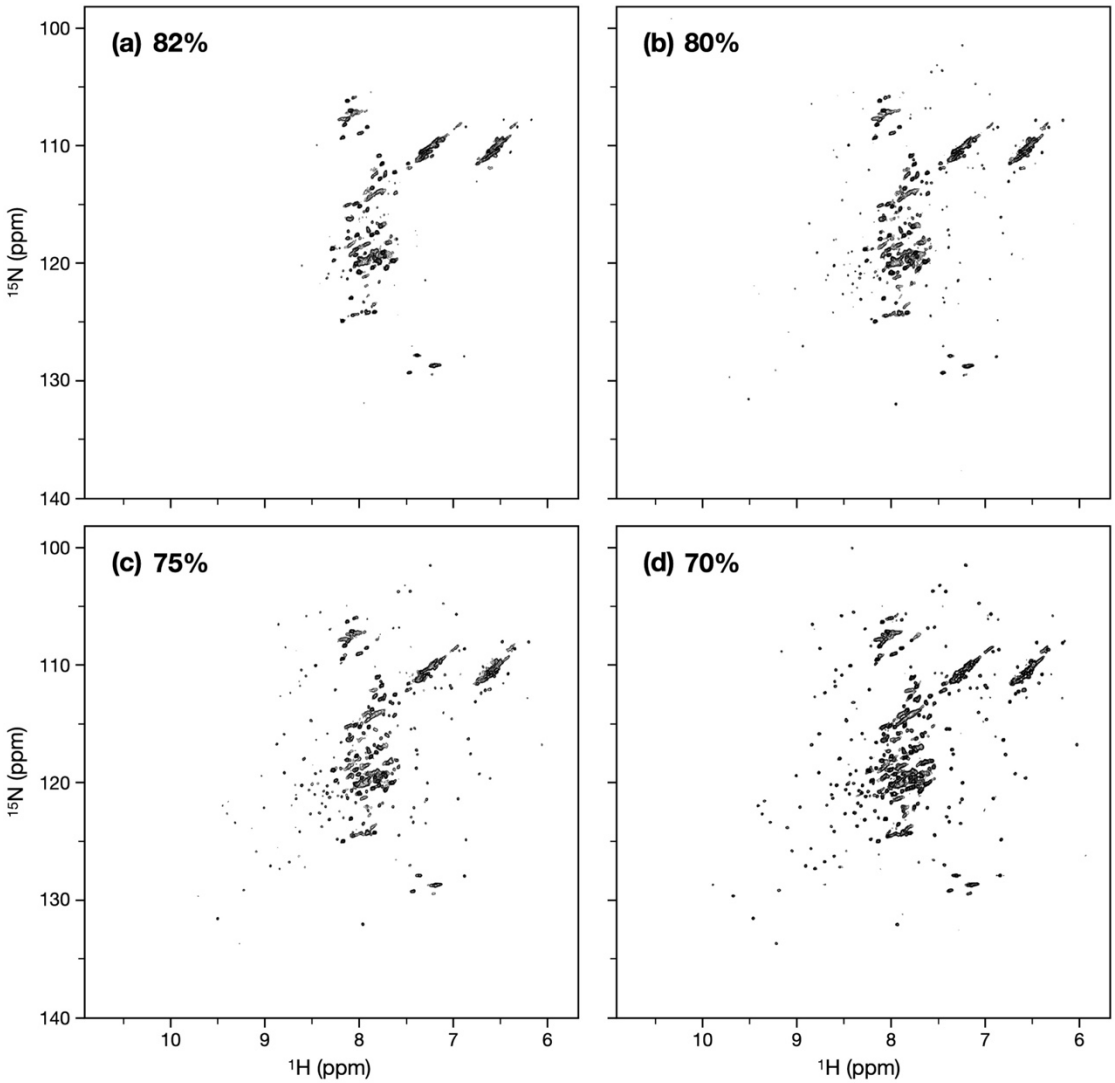

Figure S22 Refolding of CLE@2. ^{1}H–^{15}N HSQC spectra of refolding of caged CLE **2** with decreasing acetonitrile content from 84% to 70% (800 MHz, 300 K). CD_3CN/H_2O = (a) 82:18 (b) 80:20 (c) 75:25, (d) 70:30. The refolding of CLE@**2** was also almost identical to CLE@**1**. Namely, the structure remained denatured at 82% acetonitrile content, in which caged CLE has a native structure during the unfolding. The refolding began at 80%, and CLE@**2** gradually regained its native structure as acetonitrile was lowered to 70%.

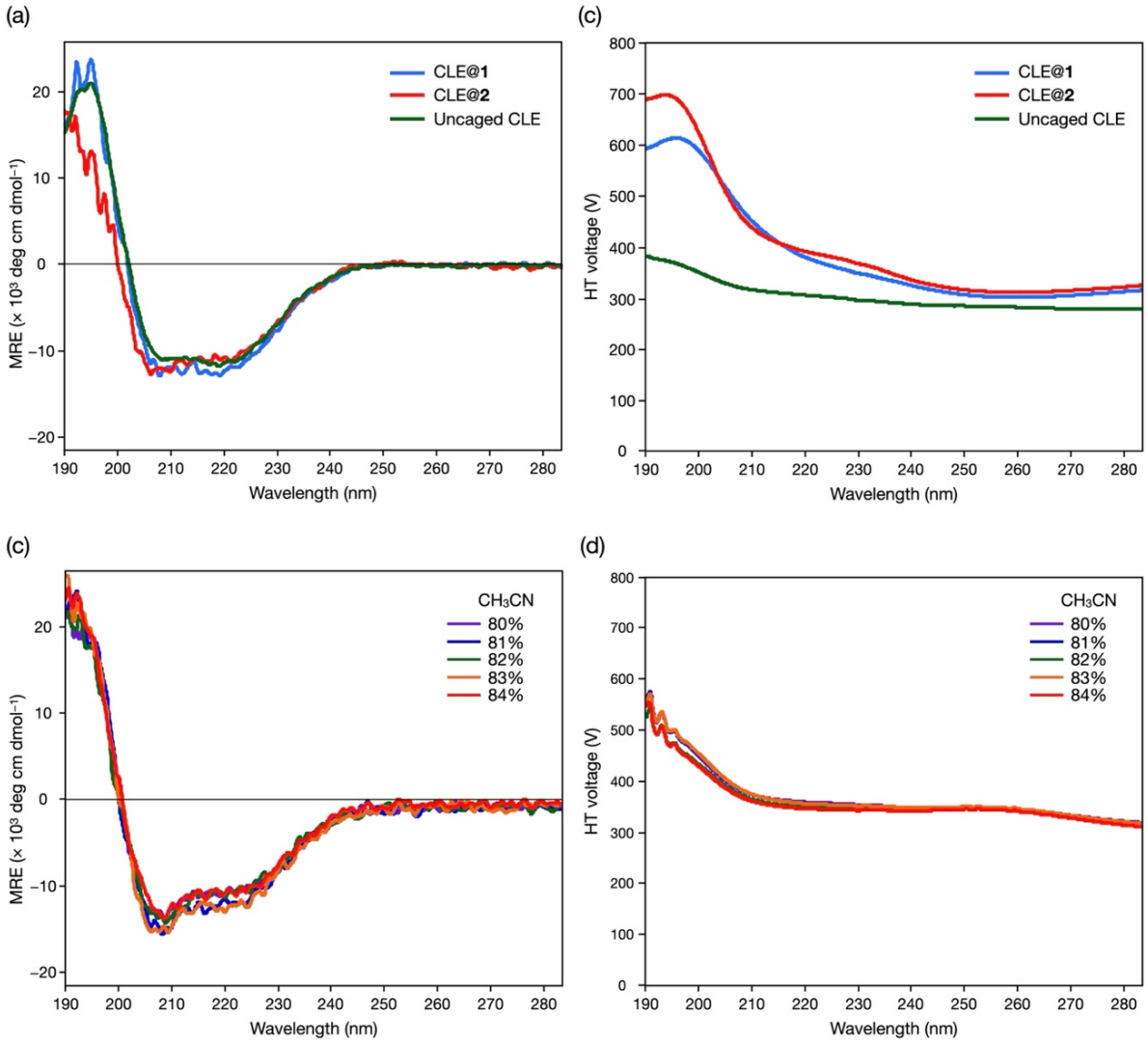

Figure S23 CD spectra of caged CLE@2. (a) CD spectra and (b) HT voltage of caged CLE **1** and **2** in acetonitrile/water = 1:1 (v/v). Both spectra of CLE@**1** and CLE@**2** well fit that of free CLE, indicating that the secondary structure was not changed through the encapsulation. The noise in the spectra of caged CLE was due to the large UV absorption of the metallo-cages. 0.072 mg/mL CLE, number of scans: 4. (c) CD spectra and (d) HT voltage of CLE@**2** in different acetonitrile/water mixtures. Caged CLE **2** also retains its secondary structure and denatured into a molten globule in high acetonitrile content. 0.036 mg/mL CLE, number of scans: 4. MRE: molar residue ellipticity.

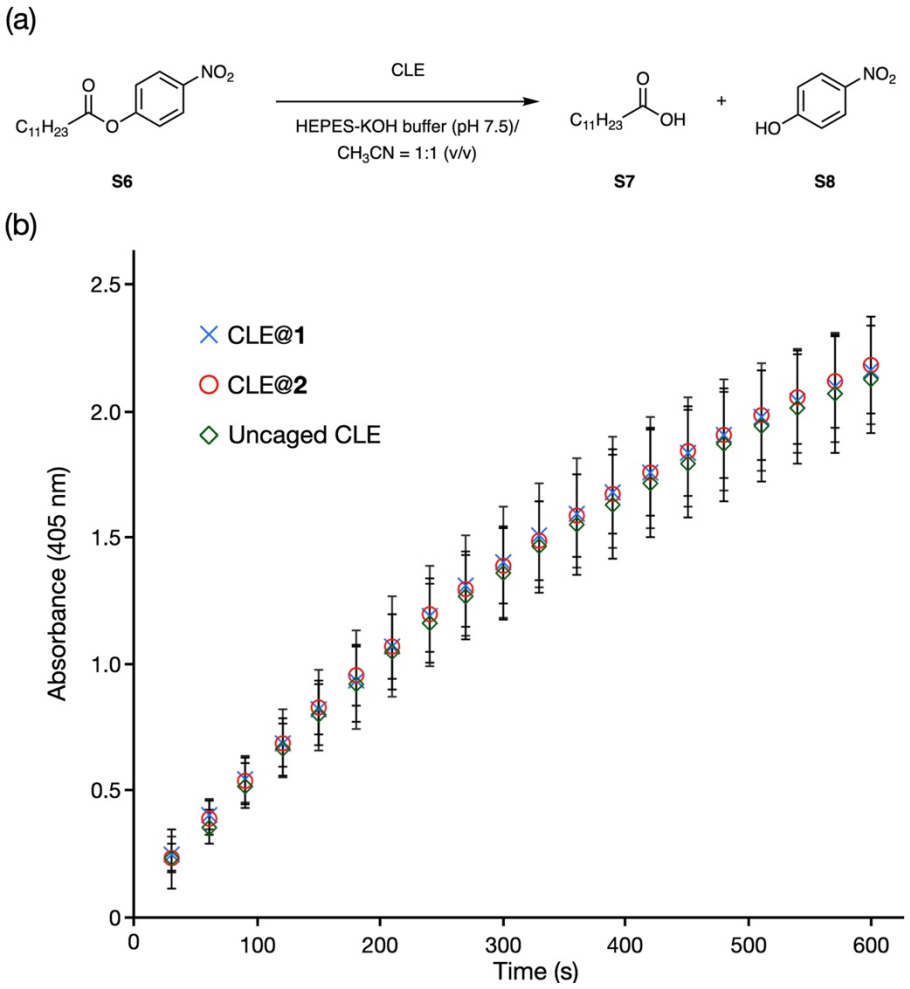

Figure S24 Enzymatic activity assay of CLE@2. (a) Schematic representation of the reaction in the activity assay. CLE hydrolyzes 4-nitrophenyl laurate (**S6**) to give 4-nitrophenol (**S8**), which has absorption at 405 nm. (b) Reaction profiles of caged CLE **1** and **2**, and uncaged CLE. n = 5. Error bars indicate standard deviation. CLE@**2** has retained the same enzymatic activity as that before the encapsulation in the self-assembled $M_{12}L_{24}$ cage.

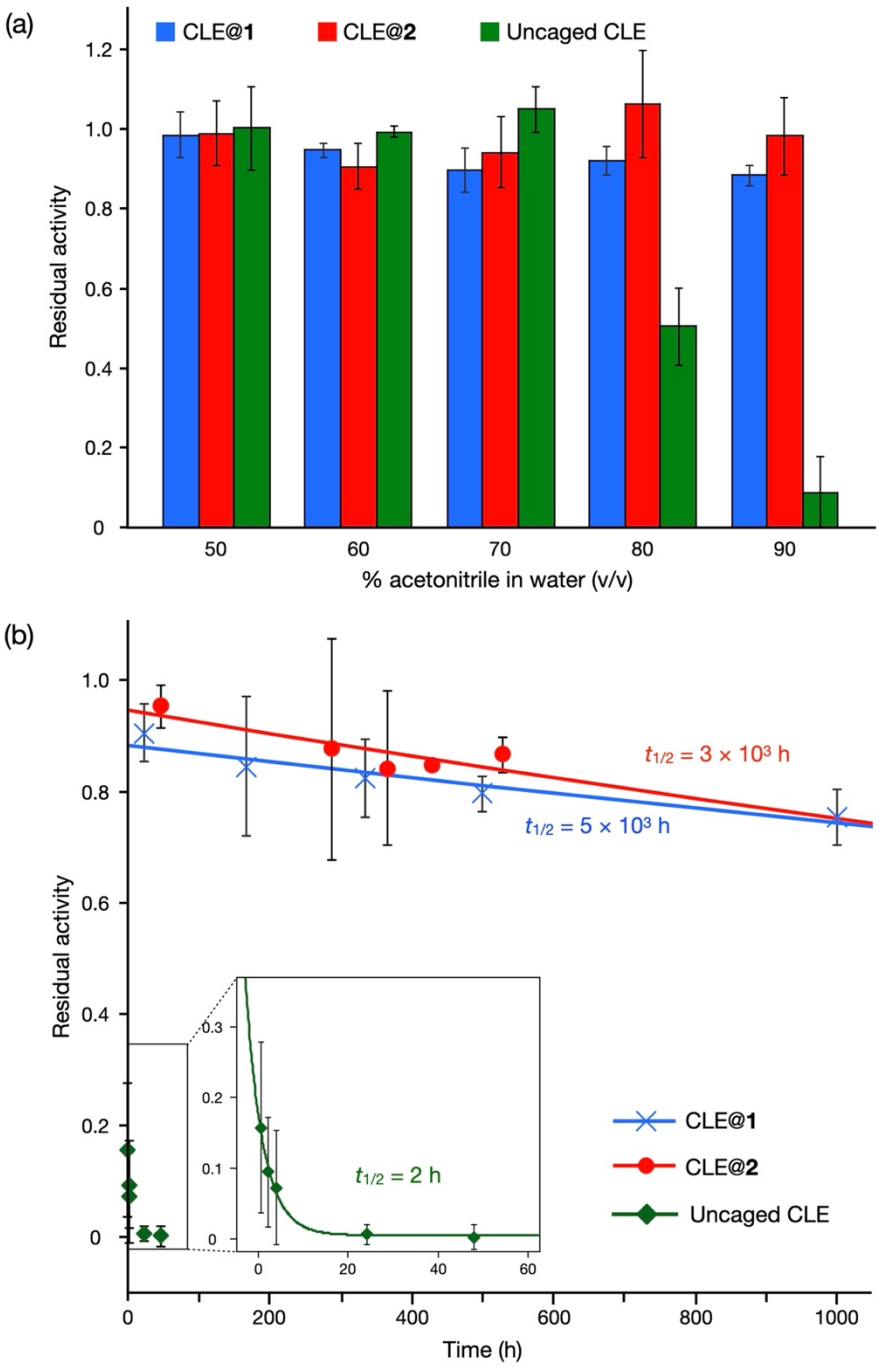

Figure S25 Stabilization of CLE via confinement in complex 2. (a) Residual activity of caged CLE **1** and **2** after exposure to different acetonitrile contents for 2 h. (b) Time course of residual activity of caged CLE **1** and **2** subjected to 90% acetonitrile (v/v) solvent. $n \geq 3$. Error bars indicate standard deviation. The activity of uncaged CLE rapidly diminished at high acetonitrile ratio (half-life in 90% CH_3CN ($t_{1/2}$) = ~2 h). In contrast, the encapsulation in both cages enhanced the stability of CLE against acetonitrile by a factor of $>10^3$. This supports that the spatial isolation stabilizes the protein regardless of the cavity size. The caged protein is prevented from aggregation under the denaturing condition and thus refolded into a native structure in the aqueous solvent used for the activity assay.

6. References

(1) W. Lee, M. Tonelli and J. L. Markley, *Bioinformatics* 2015, **31**, 1325.

(2) D. Fujita, R. Suzuki, Y. Fujii, M. Yamada, T. Nakama, A. Matsugami, F. Hayashi, J.-K. Weng, M. Yagi-Utsumi and M. Fujita, *Chem* 2021, **7**, 2672–2683.

(3) D. K. Kuila and S. C. Lahiri, *Z. Phys. Chem.* 2004, **218**, 803–828.

(4) J. W. Thompson, T. J. Kaiser and J. W. Jorgenson, *J. Chromatogr. A* 2006, **1134**, 201–209.

(5) A. N. Naganathan and V. Muñoz, *J. Am. Chem. Soc.* 2005, **127**, 480–481.

(6) M. Sakurai, *J. Chem. Eng. Data* 1992, **37**, 358–362.

(7) J. I. MacDonald, H. K. Munch, T. Moore and M. B. Francis, *Nat. Chem. Biol.* 2015, **11**, 326–331.

(8) D. Fujita, K. Suzuki, S. Sato, M. Yagi-Utsumi, Y. Yamaguchi, N. Mizuno, T. Kumasaka, M. Takata, M. Noda, S. Uchiyama, K. Kato and M. Fujita, *Nat. Commun.* 2012, **3**, 1093.